



Chinese Pharmaceutical Association
Institute of Materia Medica, Chinese Academy of Medical Sciences

Acta Pharmaceutica Sinica B

www.elsevier.com/locate/apsb
www.sciencedirect.com



REVIEW

Microfluidics for nano-drug delivery systems: From fundamentals to industrialization



Huan Zhang, Jie Yang, Rongze Sun, Songren Han, Zhaogang Yang,
Lesheng Teng*

School of Life Sciences, Jilin University, Changchun 130012, China

Received 28 October 2022; received in revised form 10 November 2022; accepted 15 December 2022

KEY WORDS

Microfluidics;
Nano-drug delivery
system;
Physicochemical
properties;
Industrialization;
Nanomedicine;
Nanoparticles;
Liposomes;
Lipid nanoparticles

Abstract In recent years, owing to the miniaturization of the fluidic environment, microfluidic technology offers unique opportunities for the implementation of nano drug delivery systems (NDDSs) production processes. Compared with traditional methods, microfluidics improves the controllability and uniformity of NDDSs. The fast mixing and laminar flow properties achieved in the microchannels can tune the physicochemical properties of NDDSs, including particle size, distribution and morphology, resulting in narrow particle size distribution and high drug-loading capacity. The success of lipid nanoparticles encapsulated mRNA vaccines against coronavirus disease 2019 by microfluidics also confirmed its feasibility for scaling up the preparation of NDDSs *via* parallelization or numbering-up. In this review, we provide a comprehensive summary of microfluidics-based NDDSs, including the fundamentals of microfluidics, microfluidic synthesis of NDDSs, and their industrialization. The challenges of microfluidics-based NDDSs in the current status and the prospects for future development are also discussed. We believe that this review will provide good guidance for microfluidics-based NDDSs.

© 2023 Chinese Pharmaceutical Association and Institute of Materia Medica, Chinese Academy of Medical Sciences. Production and hosting by Elsevier B.V. This is an open access article under the CC BY-NC-ND license (<http://creativecommons.org/licenses/by-nc-nd/4.0/>).

*Corresponding author.

E-mail address: tenglesheng@jlu.edu.cn (Lesheng Teng).

Peer review under the responsibility of Chinese Pharmaceutical Association and Institute of Materia Medica, Chinese Academy of Medical Sciences.

<https://doi.org/10.1016/j.apsb.2023.01.018>

2211-3835 © 2023 Chinese Pharmaceutical Association and Institute of Materia Medica, Chinese Academy of Medical Sciences. Production and hosting by Elsevier B.V. This is an open access article under the CC BY-NC-ND license (<http://creativecommons.org/licenses/by-nc-nd/4.0/>).

1. Introduction

In recent years, with the development of nanomedicine, microfluidics has attracted the attention of researchers all over the world, and it has been recognized as an important tool in biomedicine^{1–3}. Microfluidics is the technology that can precisely process and manipulate tiny fluids with volumes ranging from 10^{-9} to 10^{-18} L in microchannels (their dimensions are generally from tens to hundreds of micrometers)^{4–6}. Microfluidics originated in the 1990s^{2,7}, while Manz et al.^{8–10} used a chip to perform electrophoretic separation previously completed in the capillary and proposed the concept of “micro total analysis systems” (μ TAS) for the first time, which also marked the beginning of the microfluidic revolution. After that, in order to reduce the volume consumption of fluid, droplet microfluidic systems have emerged, and then digital microfluidics based on single droplet emerged in 2000. It is an alternative tool to droplet microfluidic systems which uses the electrowetting feature of droplets¹¹, where droplet microfluidic system is a technology in that tiny volume droplets can be generated by injecting dispersed phase into another continuous phase. Ever since a series of articles on microfluidics were published in “Nature” in 2006¹² and a large number of microfluidic technologies were introduced, microfluidics has been showing a rapidly developing trend². To date, microfluidics has been widely applied in various fields such as molecular detection¹³, chemical analysis¹⁴, drug evaluation^{4,15}, drug synthesis⁴, and NDDSs^{4,16,17}, etc. NDDSs are pharmaceutical formulations with a particle size of 10–1000 nm, consisting of drugs and functional drug nanocarriers prepared from biocompatible and/or biodegradable materials^{2,6,18}. They can deliver drugs to the desired site and realize the drugs’ sustained release, thereby reducing drugs’ toxicity and improving drugs’ bioavailability². Various NDDSs, such as liposomes, nanoparticles, and micelles, have been extensively studied and hold great promise in the treatment of various diseases including tumors^{19–22}, diabetes²³, and asthma^{24,25}. Usually, NDDSs are prepared by bulk methods including, but not limited to, homogenization, self-assembly, and nanoprecipitation. These traditional methods result in wide particle size distribution, poor dispersion, and high batch-to-batch variations in physicochemical properties²⁶, mainly owing to low mixing efficiency and slow mass transfer. These shortcomings strongly affect clinical results^{27–29}, which is one of the main reasons for the slow clinical translation of NDDSs²⁸.

Microfluidics offers a new strategy for fabricating NDDSs^{26,30}. It can precisely process and manipulate tiny fluids in the microchannel, resulting in some features including small volume, large specific surface area, and fast mass and heat transfer, which brings about remarkable advantages such as low consumption of reagents, fast mixing, and precise control of the physicochemical properties of NDDSs^{4–6}. According to the properties of fluid phases, microfluidics is divided into two categories: continuous-flow microfluidics and segmented-flow microfluidics³¹. The continuous-flow microfluidics mainly focuses on miscible fluid, while segmented-flow microfluidics focuses on two-phase fluid where it introduces an immiscible liquid or gas into a miscible liquid to produce a regularly spaced segmented interface. Both these two categories of microfluidics can continuously control the reaction condition, process parameters (*e.g.*, FRR, flow rate, chip geometry, and temperature) and the mixing sequence of reagents during the reaction process, achieving controllable preparation of NDDSs²⁹. Theoretically, the physicochemical properties of NDDSs including particle size, distribution, and morphology of

NDDSs can be well controlled by microfluidic technology³², and the scheme is presented in Fig. 1.

Furthermore, microfluidics can scale up the production of NDDSs for clinical application *via* parallelization or numbering-up^{4,16}. LNPs-encapsulated mRNA vaccines (BNT16b2 and mRNA-1273) for COVID-19 have been successfully produced using microfluidics by Pfizer–BioNTech and Moderna^{16,33}, which not only prevent severe cases of COVID-19 worldwide but also demonstrate the feasibility of microfluidics for scaling up the preparation of NDDSs. In view of this, a detailed depiction of microfluidics-mediated NDDSs from fundamentals to industrialized applications is of great importance. Thus, herein we present a comprehensive review of microfluidics-mediated NDDSs. Firstly, we summarize the fundamentals of microfluidics which includes fluid characteristics, fluid mixing, and manipulation. Secondly, the microfluidic synthesis of NDDSs is presented. Finally, the industrialization and challenges of microfluidics-mediated NDDSs in the current status are discussed.

2. The fundamentals of microfluidics

2.1. The materials for microfluidic devices

Microfluidic devices play an important role in fabricating NDDSs. Therefore, the material for microfluidic devices is critical since the wetting and contact angles of the solution maybe also affect the properties of NDDSs⁴. Recently, various materials including silicon, glass capillary, paper, and PDMS have been applied to fabricate microfluidic devices². We summarized the pros and cons of commonly used material for microfluidic devices, as shown in Table 1^{2,4,9}.

Glass and silicon are the earliest materials for the fabrication of microfluidic devices. Glass materials have the advantages of transparency and insulation, high thermal conductivity and stable electro-osmotic mobility. Moreover, it can be easily assembled into a capillary device. Glass capillary can provide a three-dimensional axisymmetric fluid channel where the fluids are not in contact with the channel inner wall, increasing the production efficiency of NDDSs. Silicon materials show the features of well chemical compatibility and thermostability, high design flexibility and semiconductive⁹. Microfluidic devices fabricated by silicon materials can sustain high temperatures and pressures. However, some limitations including opacity and fragility still affect its application in the fabrication of NDDSs. To avoid the aforementioned drawbacks, researchers are switching to PDMS-based microfluidic devices in recent years, due to their advantages of cheap, high optical transparency, excellent biocompatibility and high elasticity. However, they can be easily deformed and corroded by organic solvents, which will affect the physicochemical properties of NDDSs. Therefore, in order to meet the needs for fabricating NDDSs, some essential factors such as chemical compatibility, durability, and transparency must be also taken into consideration.

2.2. Fluid characteristics in microfluidic devices

Generally speaking, the fluidic regime is mainly divided into laminar and turbulent flow⁷. In laminar flow, the fluid flows in parallel layers and the velocity of the fluid at any location is constant, while turbulent flow shows no distinct streamlines, as presented in Fig. 2.

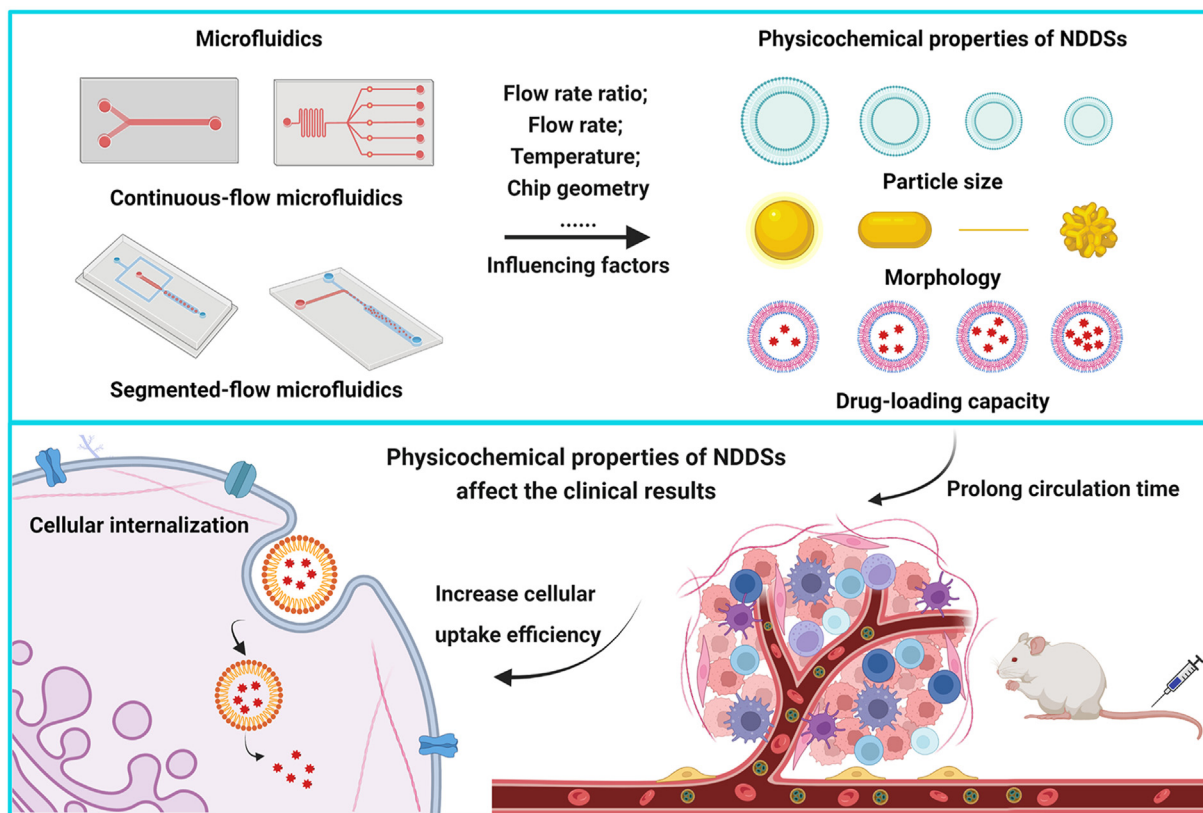


Figure 1 The impact of microfluidics on the physicochemical properties of NDDSs, and the influences of NDDSs with different structures on experimental results *in vivo*. Microfluidics is divided into continuous-flow microfluidics and segmented-flow microfluidics. The physicochemical properties of NDDSs (e.g., particle size, morphology, and drug-loading capacity) can be well-controlled by continuously monitoring the reaction condition and process parameters such as FRR, flow rate, temperature and chip geometry. And the circulation time was prolonged and cellular uptake efficiency was increased.

R_e as an important parameter can be used to reflect fluid regime². R_e stands for the relative magnitude of inertia and viscous forces of the fluid and it can be calculated by Eq. (1)^{30,34}:

$$R_e = \frac{\rho u D_h}{\mu} \tag{1}$$

where ρ stands for fluid density, u and μ are the average fluid velocity and dynamic viscosity, respectively. D_h is the hydraulic

diameter of the microfluidic channel, which is related to the cross-section area and wet perimeter of the channel^{30,34}.

At low R_e (<1800), viscous forces play a dominant role, and a laminar flow occurred³⁰. The fluid flows in a parallel layer and fluid velocity at any location is constant. In this situation, the mass transfer can only occur in the direction of fluid flow and passive molecular diffusion is dominant⁴. Whereas at high R_e (>2000), inertia force is dominant and turbulent flow without distinct streamlines is occurred², and the mass transfer occurs in all spatial

Table 1 The pros and cons of materials for microfluidic devices.

Material	Pros	Cons
Silicon	Well chemical compatibility and thermostability; Ease of fabrication; High design flexibility; High insulation.	High opacity; Fragile; High cost.
Glass	High transparency and insulation; High thermal conductivity; Stable electro-osmotic mobility.	Expensive to be manufactured into chips; Time-consuming; Low production efficiency.
PDMS	Low cost; High optical transparency; Excellent biocompatibility; High elasticity.	High organic solvent swelling rate; Easy deformation.

PDMS, poly(dimethylsiloxane).

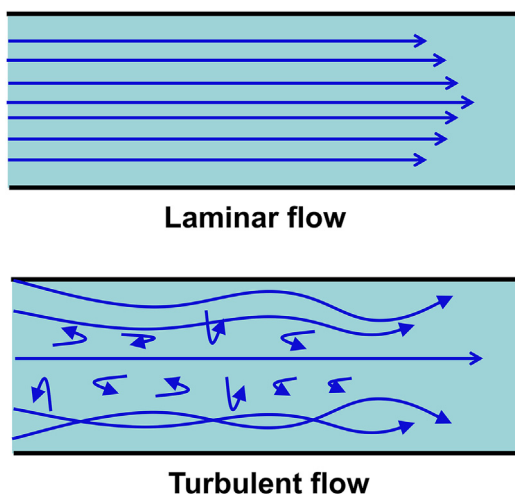


Figure 2 The schematic diagram of two fluidic regimes. The fluid flows in parallel layers and the velocity of the fluid at any location is constant in laminar flow, while turbulent flow shows no distinct streamlines.

directions. The transition state ($1800 < Re < 2000$) generally occurs between laminar and turbulent^{35,36}.

From Eq. (1), we can know that the fluidic regime is related to fluid density, fluid velocity, dynamic viscosity, cross-section area and wet perimeter of the channel. A low Re number can be obtained by increasing the dynamic viscosity of fluids or decreasing fluid density and/or fluid velocity and/or the hydraulic diameter of microfluidic channel^{2,4,37}. The dimensions of microfluidic channels are usually in the micrometer range, so lower Re can be obtained. Re is extremely low ($Re < 100$) in microfluidic devices, and laminar flow can be achieved^{29,30}. Because laminar flow shows steady streamlines, fluids in the microfluidic device can be precisely manipulated and the mass transfer is dominated by passive molecular diffusion and advection in microfluidic device⁴. Molecular diffusion can be explained by Brownian motion, that is, molecules transport from higher concentration to lower concentration, resulting in a gradual mixing between precursors.

P_e as another important parameter can reflect molecular diffusion³⁸. P_e reflects a relative magnitude of convection rate and diffusion rate³⁹. When P_e is low, molecular diffusion is dominant^{2,4,37}. P_e can be calculated by Eq. (2)³⁸:

$$P_e = \frac{uL}{D} \quad (2)$$

where u and L are fluid velocity and diffusion distance, respectively. D stands for the diffusion coefficient of fluid³⁸. As shown in Eq. (2), P_e is positively related to fluid velocity and diffusion distance^{35,36}. Fluids in microfluidic channels usually have a larger P_e . In immiscible liquids, molecular diffusion is relatively difficult in the microfluidic channel and liquid–liquid interfaces can be obtained, while for a miscible solution, an interface can also be formed, and molecular diffusion can occur laterally or longitudinally². The transfer of molecules from one liquid to another is minimized, resulting in higher drug-loading capacity⁷.

2.3. Microfluidic mixing in microfluidic devices

Mixing efficiency or mixing time between precursors plays a critical role in controlling the physicochemical properties of

NDDSs. Higher mixing efficiency or shorter mixing time can achieve the smaller, more uniform particle sizes and excellent dispersity of NDDSs. The molecular diffusion time (t) over the distance can be calculated by Eq. (3)³⁰:

$$t = \frac{L^2}{2D} \quad (3)$$

where L and D are the same as Eq. (2). The molecular diffusion time is positively related to diffusion distance and negatively correlated with the diffusion coefficient of fluid. A shorter molecular diffusion time can be realized by reducing diffusion distance. In general, the diffusion coefficient of water-soluble molecules such as ions or dyes is 10^{-9} m²/s, and their molecular diffusion takes 5 s when the diffusion distance is $100 \mu\text{m}$ ⁴⁰.

In order to improve mixing efficiency between precursors, various microfluidic devices have been designed, such as microfluidic chips with different geometries, three-dimensional hydrodynamic flow focusing microfluidic devices, multi-inlet vortex mixer and confined impinging jets mixer, etc. According to their different mixing mechanisms, the microfluidic mixing strategy is classified as active microfluidic mixing and passive microfluidic mixing⁴¹. In active microfluidic mixing, external energy sources such as pressure, ultrasonic, temperature, electricity were applied to perturb precursors and improve their mixing efficiency³⁰. The introduction of external energy sources endows a higher mixing efficiency than passive microfluidic mixing. However, the use of an external energy source may increase the samples' temperature, thus destroying their biological activity. Therefore, active microfluidic mixing is not particularly suitable for pharmaceutical and biological applications.

Passive microfluidic mixing does not require external energy sources and relies entirely on the fluid pump and special structure of the microfluidic channel to increase contact surface area and reduce diffusion distance³⁰. Many passive microfluidic devices had been developed over the past 30 years. For instance, T- and Y-shaped microfluidic chips, which are the simplest microfluidic devices, were developed to improve mixing efficiency though they need a relative long mixing channel between mixing fluids. To overcome this shortcoming, split and recombined structures were introduced so that the fluids can be immediately split into many layers and finally recombined into one layer, which can effectively improve mixing efficiency. Nowadays, this strategy has been widely applied in drug delivery systems^{36,48,49}.

2.4. Microfluidic liquid manipulation

According to the properties of the fluid phases and the interfaces, microfluidic liquid manipulation can be divided into two main categories: continuous-flow microfluidics and segmented-flow microfluidics³¹. Owing to rapid mass transfer and precisely manipulating microfluidic liquid, both fluid manipulation categories can be applied to fabricate NDDSs with narrow particle size, higher drug-loading capacity, excellent dispersion and repeatability. In this section, we describe these two strategies in detail.

2.4.1. Continuous-flow microfluidics

The continuous-flow microfluidics is also called single-phase continuous-flow microfluidics, which mainly focusing on miscible fluid³⁶. Its principle is very simple: a dynamic and diffusive interface can be formed in miscible fluid while two fluids are gradually mixed. During this process, the reaction occurs in

the diffusion region³⁸. The reactant composition along the reaction channel can be continuously varied, which results in high yield of NDDSs⁴. Owing to the simplicity of the flow pattern, the scale-up of NDDSs can be realized by simply increasing the flow rate⁴².

HFF is one of the most common continuous-flow microfluidics that can be applied for the preparation of NDDSs by using flow focusing of miscible fluids on microscale platforms^{36,43}. Depending on their structure, it is usually divided into 2D-HFF and 3D-HFF. In general, 2D-HFF is focused on the horizontal direction and achieved by introducing two inlets of non-solvent as the sheath liquid to horizontally confine the precursors solvent in the central inlet⁴⁴. The diffusion distance can be significantly shortened owing to the confinement of sheath liquid for precursors solvent, thus the mixing time is further reduced⁴⁵ (the scheme is shown in Fig. 3A⁴⁴). Higher mixing efficiency leads to the smaller, more uniform particle size and excellent dispersity of NDDSs. Therefore, in order to further improve mixing efficiency between reagents, 3D-HFF was developed (as presented in Fig. 3B⁴⁶). The liquid is focused horizontally and vertically into tiny fluids⁴⁶. Compared with 2D-HFF, 3D-HFF can isolate the precipitation polymer from the channel walls, mix precursors more efficiently, thus no channel fouling occurred⁴⁷. Moreover, 3D-HFF can also

control the particle size distribution and polydispersity of NDDSs⁴³.

In a microfluidic device, fluid mixing is achieved through molecular diffusion and the reaction environment is relatively stable and mild. However, in some situations, this mixing strategy is time-consuming and insufficient. In order to solve these problems, microfluidic devices with chaotic mixers were developed to induce transverse flow and reduce the mixing distance. They possess a complicated three-dimensional grooved mixer structure. Chaotic advection in the microchannels can be generated by local rotational and extensional flows, thereby the mixing efficiency between precursors is rapidly enhanced³⁴. Structures of chaotic mixer are presented in Fig. 3C and D^{34,42}. Many microfluidic devices with chaotic mixers such as herringbone and Tesla had been developed to improve mixing efficiency³⁶. Our group also fabricated a 3-inlets microfluidic chip with polydimethylsiloxane/glass by conventional UV photolithography and soft-lithography⁴⁸. This microfluidic device with herringbone structure and S-type channels with a depth of 70 μm and a width of 200 μm excellently improved the mixing efficiency between lipid solution and siRNA solution. Additionally, we also designed an inverted W-type microfluidic chip, in which the mixing efficiency between

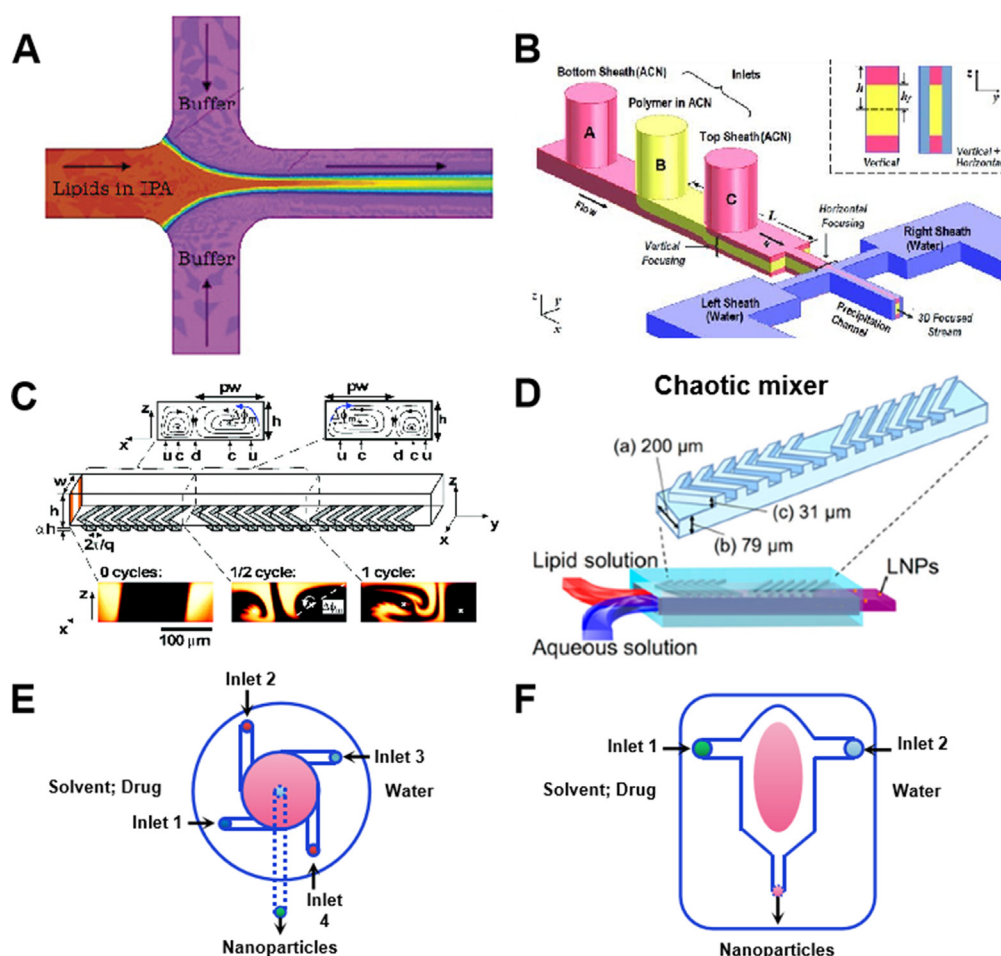


Figure 3 Continuous-flow microfluidics. (A) 2D-HFF microfluidics (Reprinted with the permission from Ref. 44. Copyright © 2004 American Chemical Society); (B) 3D-HFF microfluidic device (Reprinted with the permission from Ref. 46. Copyright © 2011 Wiley-VCH); (C, D) microfluidic device with chaotic mixer (Reprinted with the permission from Refs. 34 and 42. Copyright © 2004 American Chemical Society; Copyright © 2018 American Chemical Society); (E) multi-inlet vortex mixer; (F) confined impinging jet mixer.

the outer aqueous phase and the internal organic phase was significantly improved⁴⁹.

The cycle number of a chaotic mixer and its structure parameters such as depth, width, and height all play an important role in improving mixing efficiency⁵⁰. The size distribution of NDDSs can be tuned by controlling the cycle number of a chaotic mixer. The appropriate cycle number of a chaotic mixer can obtain a narrower size distribution of NDDSs⁵¹. In general, a deeper chaotic micromixer structure can achieve a higher mixing efficiency⁵². Of course, there are some exceptions since deeper chaotic micromixer structures may lead to a clogged problem, resulting in stagnation of sample flow. It is important to point out that the clogged problem must be addressed though the microfluidic devices with chaotic mixers can improve mixing efficiency between reagents^{36,42}. Additionally, the concentration of the precursors, flow rate and FRR, etc.^{51,52}, should also be taken into consideration which can provide some help for the design of the microfluidic device.

Multi-inlet vortex (Fig. 3E) is also able to improve mixing efficiency between reagents to realize the rapid precipitation of organic compounds. Lots of polymeric nanoparticles can be high-throughput produced by controlling fluid velocity⁵³. Moreover, confined impinging jets (Fig. 3F) can very efficiently alter the organic nucleation and growth of particles, further tuning their average particle size and size distribution⁵³.

2.4.2. Segmented-flow microfluidics

Segmented-flow microfluidics introduces an immiscible liquid or gas into a miscible liquid to produce a regularly spaced segmented interface (liquid–liquid or gas–liquid). Droplet microfluidics, one of the segmented-flow microfluidics, was widely applied to fabricate NDDSs⁴. It is a technology in that tiny volume droplets can be generated by injecting one liquid phase (the dispersed phase) into another immiscible or partially immiscible liquid phase (the continuous phase) and sheared off at the junction where two phases meet⁵⁴. One of the most outstanding advantages of droplet microfluidics is its ability to produce monodisperse droplets with a narrow size distribution⁵⁵. In a microfluidic system, the size of droplets often varies from several to hundreds of microns, and their coefficient of variation is normally below 5%⁴. The size of droplets can be precisely controlled by tuning the geometry of microfluidic devices, the properties of two liquid phases, and the operating parameters including flow rates, temperature, FRR, etc., thus providing a reliable way to fabricate NDDSs with uniform sizes and different structures⁵⁵.

Various geometries of the microfluidic device have been designed for generating droplets, including T-junction, flow-focusing, and coaxial structure, etc.^{4,41}. A T-shaped chip is the simplest and mostly used structure for droplet formation, as shown in Fig. 4A. The continuous phase is injected into the main channel and the dispersed phase is injected into the vertical channel. The water–oil interface is generated at the junction and droplets are obtained. The diameter of droplets can be controlled by varying fluid flow rate, channel dimension, and the interfacial tension between two phases. In a coaxial-focusing structure, the channel of the dispersed phase is concentrically placed inside the continuous phase channels. When the dispersed phase and continuous phase are injected, the dispersed phase is surrounded and sheared by the continuous phase to form droplets, as shown in Fig. 4B. The dimension and generation frequency of droplets are affected by fluid properties and velocity. The flow-focusing structure includes three injection branches, in which two branches are

continuously and symmetrically injected into continuous phase to shear dispersed phase. Droplets are formed at the rear end of the intersection of three branches, as shown in Fig. 4C. Similarly, the characteristic of the droplet is affected by fluid flow rate and the channel dimension.

Droplets can be formed in three main regimes: dripping, jetting, and stable co-flow⁵⁶, as shown in Fig. 4. C_a can be used to reflect droplets' regimes, and it stands for the relationship between viscous force and interfacial tension, which can be calculated by Eq. (4)¹:

$$C_a = \frac{\mu v}{\gamma} \quad (4)$$

where μ , v , and γ stand for the viscosity of the continuous phase (kg/m·s), shear rate (m/s), and interfacial tension between the continuous and dispersed phases (N/m), respectively. When the C_a value is extremely low, the dispersed phase hinders the continuous phase, and droplets are formed by dripping. With the increase in C_a value, the viscous shear force overcomes the interfacial tension, and the droplet regime presents jetting. While when C_a value is further increased, droplets are broken in the channel, showing a stable co-flow regime. As shown in Eq. (4), droplet regimes can be changed by adjusting the viscosity of the continuous phase and flow rate. At a low flow rate, a dripping regime is observed; while the jetting regime is presented by increasing the flow rate, and polydisperse droplets are produced. Dripping regime was widely applied to fabricate NDDSs.

Droplet microfluidics is able to precisely control the fluid behaviors, therefore, droplets with different dimensions and morphologies can be formed. Droplets are usually classified as single-emulsion droplets, double-emulsion droplets, multi-emulsion droplets, and multiple cores' droplets⁴, as presented in Fig. 4D. Single-emulsion droplets consisting of two immiscible liquids are the simplest structure. According to the difference between the dispersed phase and continuous phase, four typical types (e.g., W/O, O/W, W/W, and O/O) had been developed to synthesis of NDDSs⁴. The size of single-emulsion droplets can be well-controlled by adjusting the flow rate or the structure of the microfluidic device. Moreover, the throughput production of emulsion droplets can be enhanced by parallelizing the microfluidic device, which allows mass production of NDDSs⁵⁷. Double emulsion droplets are usually dispersed drops containing smaller drops inside, which had been widely used to fabricate NDDSs with core/shell structure, while the outer and inner droplets become the shell and core of NDDSs, respectively¹. By adding the number of microfluidic devices, double-emulsion droplets can be produced by further encapsulating simple emulsion droplets. Czekalska et al.⁵⁸ fabricated a double emulsion device by extending a microfluidic device with a flow-focusing junction. W/O droplets were firstly formed in the first junction, and then encapsulating W/O droplets at the second junction to form a W/O/W double emulsion. Meanwhile, the size of droplets can be specifically controlled by simple varying the osmotic gradient. Thus, multi-emulsion with uniform particle sizes can be achieved by the one-step method. The generation process of multi-emulsion droplets is similar to that of double-emulsion droplets. Multi-emulsion droplets have more complex nested systems in which lots of small size droplets are placed inside another droplets. Besides, droplets with multiple cores can be obtained by tuning the flow rate of each fluid phase. Therefore, the number and components of inner compartments of the droplet can also be strictly controlled⁴.

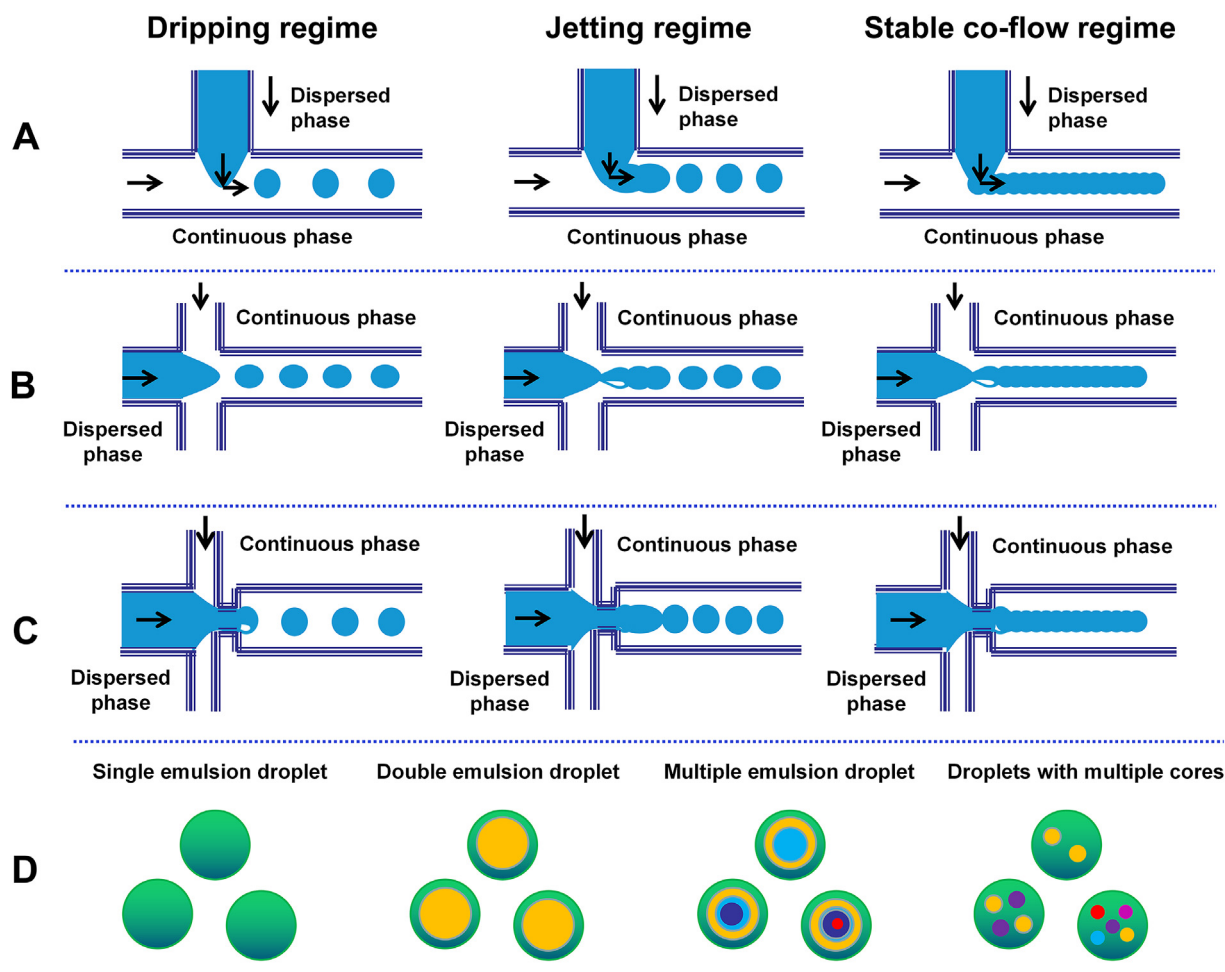


Figure 4 The structure of droplet microfluidic device, droplet regimes, and the morphologies of droplets generated from microfluidics. (A) T-junction; (B) co-flowing junction; (C) flow-focusing junction; (D) the morphologies of droplets including single emulsion, double emulsion droplet, multiple emulsion droplet and droplets with multiple cores.

In summary, microfluidics provides a new strategy for fabricating NDDSs with narrow particle size, excellent dispersity, and high drug-loading capacity owing to its excellent properties such as laminar flow, rapid mass transfer, and high mixing efficiency. It can be manipulated as continuous-flow microfluidics and segmented-flow microfluidics. The physicochemical properties of NDDSs can be controlled by tuning FRR, flow rate, and the structure of microfluidic device (*e.g.*, width, depth, the height of the channel). Higher FRR or flow rate can achieve the smaller particle size and excellent dispersion of NDDSs. Higher mixing efficiency between precursors can produce a narrower size distribution of NDDSs, which provides a guide for synthesis and industrialization of microfluidics-mediated NDDSs.

3. Microfluidic synthesis of NDDSs

NDDSs possess multiple advantages, such as targeting, sustained release of drugs, low drug toxicity and high bioavailability, etc.². Microfluidics as a suitable method for fabricating NDDSs can elaborately control fluids to achieve effectively mixing between different reagents in a highly uniform and orderly manner.

Therefore, a large variety of microfluidics-mediated NDDSs (*e.g.*, liposomes, nanoparticles, micelles) have been extensively developed in recent years. Some important examples are summarized in Table 2^{49,56,59–86}. In this review, according to their physicochemical properties, the commonly used NDDSs are discussed: liposomes-based NDDSs; nanoparticles-based NDDSs including LNPs, inorganic nanoparticles, protein nanoparticles, and PNPs.

3.1. Liposomes-based NDDSs

Liposomes are a type of lipid vesicles with a phospholipid bilayer and an aqueous core^{87,88}. Owing to their high biocompatibility, good stability, sustained release and high cellular uptake, liposomes as drug carriers have been widely investigated^{89–92}. Microfluidics for fabricating liposomes-based NDDSs usually includes a fluid focusing method and droplet microfluidics^{93,94}. Among all these microfluidics used for liposomes-based NDDSs preparation, the most commonly used method is the fluid focusing method based-on continuous flow microfluidics. In this method, the formation of liposomes can be controlled by molecular diffusion of interface substances between miscible liquids⁹⁵. Meanwhile, their average size and dispersion can also be tuned by

adjusting the flow velocity of aqueous solution⁹⁶. Jahn et al.⁴⁴ was the first to demonstrate the synthesis of liposomes by 2D-HFF. In their work, the lipid solution containing a fluorescent dye (DiIC18) and PBS was introduced into a microfluidic chip which was composed of a cross-type glass and silicone microchannel with 200- μm width and 40- μm depth. A narrow mixing solution region was formed inside the chip and liposomes with a particle size of 100–300 nm were obtained by squeezing of water-to-lipid phase. Subsequently, the influencing factors of liposome synthesis were further studied in their other works. For example, Jahn et al.⁹⁶ fabricated two different channel dimensions of 2D-HFF devices to investigate the effect of FRR on the average size of liposomes. Numerical simulations of microfluidic device design and HFF is shown in Fig. 5A⁹⁶. It demonstrates that the mixing and surface-to-volume ratio of the focused IPA stream in both channel geometries increases with the increase of FRR. A higher FRR could produce smaller-sized liposomes with narrow size distribution. In another word, the rapid mixing of reagents enables the produce of small-sized and narrow-particle-size-distributed NDDSs⁹⁶. Furthermore, some other researches^{63,97} also showed that lipid concentration plays important roles in controlling the particle size and productivity of liposomes-based NDDSs.

Although 2D-HFF can excellently control the dispersion and particle size of liposomes-based NDDSs, a slow flow rate will lead to a lower production throughput, therefore limiting their scale-up⁹⁷. In order to solve this problem, Chen et al.⁹⁸ designed a high-aspect-ratio fluid-focusing channel with high-resolution 3D printing technology to support large-volume flow and the scheme of the technique is presented in Fig. 5B⁹⁸. With this technique, high-throughput production of liposomes can be achieved with the productivity of up to 4 mg/min.

Microfluidic system also contributes greatly to the drug-loading of liposomes, especially in the encapsulation of nucleic acid drugs⁶⁴. Microfluidics can not only reduce the degradation of nucleic acids but also improve their mixing efficiency, resulting in a more uniform mixture between lipids and nucleic acid drugs. Balbino et al.⁹⁹ prepared liposomes-based NDDSs (pDNA/CL) by multiple hydrodynamic focusing regions (the scheme is presented in Fig. 5C⁹⁹). In their work, microfluidic platform with two different regions was designed. After the synthesis of the empty liposomes, liposomes and pDNA were directly assembled, and this simplifies the tedious steps in the traditional method. The transfection results *in vitro* showed that the transfection efficiency of liposomes prepared by a microfluidic platform is similar to those fabricated by a conventional method. Liposomes co-loaded with multiple drugs including genetic drugs can also be obtained by increasing the number of microfluidic device geometry or modifying the microfluidic chip¹⁰⁰. Zhang et al.¹⁰¹ designed a multi-stage microfluidic chip to prepare liposomes co-loaded with siRNA and DOX. siRNA and DOX were encapsulated in different regions of a multistage microfluidic chip, which simplifies the tedious drug-loading process and saves preparation time.

Droplet microfluidics, which can be divided into the single-emulsion droplet method and double-emulsion droplet methods, is also used to prepare liposomes-based NDDSs¹⁰². The double-emulsion droplet method which uses W/O/W as the standard method is one of the most common methods to prepare liposomes¹⁰³. Its principle is very simple, namely, volatile organic reagents were used as oil phase to accelerate the distribution of lipids solution at the W/O interface. Subsequently, a double-emulsion can be formed¹⁰⁴. In general, liposomes-based NDDSs generated by droplet microfluidics possess higher encapsulation

efficiency. Moreover, their particle size and monodispersity can be more precisely controlled¹⁰⁵.

3.2. Nanoparticles-based NDDSs

Nanoparticles are solid colloidal particles made of natural or synthetic materials with a particle size in the nanometer order¹⁰⁶. Owing to the difference in the raw materials used, nanoparticles are divided into different types: LNPs, PNPs, protein nanoparticles, and inorganic nanoparticles¹⁰⁷. Therefore, in this review, we focus on their preparation by microfluidics.

3.2.1. Lipid nanoparticles

LNPs are one of the most widely studied NDDSs. They possess lipid-encapsulated shells and oily, solid, or amorphous cores^{108–110}. In LNPs, the incorporation of lipids helps to overcome the burst release and reticuloendothelial absorption of the drug in the nanoparticles. They present many advantages including excellent sustained release^{111,112}; good biocompatibility^{113,114} and high stability *in vivo*^{115–118}. LNPs also can load all kinds of drugs owing to their superior properties. Hydrophilic drugs are encapsulated into the aqueous phase, while hydrophobic drugs are encapsulated into the lipid phase; amphiphilic drugs can be inserted into lipid membranes^{119,120}. Moreover, both hydrophilic and hydrophobic drugs can also be simultaneously encapsulated into LNPs¹²¹. Compared with liposomes, LNPs can more stably encapsulate nucleic acid drugs¹²². Therefore, LNPs play an important role in the prevention and treatment of infectious diseases¹²³, cancer¹²⁴ and hereditary diseases¹²³.

Continuous-flow microfluidics is the most used method to fabricate LNPs-based NDDSs. It is able to provide on-demand and tailored synthesis¹²⁵. This method is simple, where a lipid solution is dissolved in an organic solvent and an aqueous solution is introduced into the microfluidic device. The lipid stream is squeezed by an aqueous solution stream, and LNPs are produced at the liquid–liquid interface with the dilution of lipid solution¹²⁶. Arduino et al.⁶⁹ prepared LNPs by nano precipitation in a glass capillary microfluidic device. During precipitation, the internal and external solutions, consisting of a lipid matrix dissolved in a 95% ethanol solution and an aqueous solution containing a stabilizer, are pumped into a microfluidic device at a constant flow rate in the same direction. It was found that LNPs prepared by this method were superior to the traditional methods in morphology, size and PDI. The experimental results *in vitro* have confirmed that LNPs-based NDDSs produced by microfluidics have a stronger cytotoxicity on cancer cells than free drugs.

The properties of LNPs are greatly influenced by the particle size and their size distribution^{127,128}. Flow rate, FRR, and lipid concentration are the important parameters to control the physicochemical properties of LNPs¹²⁹. Roces et al.⁶⁷ found that LNPs with different sizes and dispersity could be obtained by changing the ratio between cholesterol and cationic lipids. Okuda et al.⁷⁰ revealed that salt concentration could significantly affect the particle size of LNPs. By adding appropriate salt to the buffer of nucleic acid to increase the particle size of LNPs, the obtained LNPs with the larger particle size showed higher gene expression efficiency and better therapeutic effect. Hood et al.⁴³ fabricated a 3D-HFF device assembled from seven identical borosilicate glass capillaries in a large capillary to synthesize LNPs. In this 3D-HFF microfluidic device, each capillary possesses an inner diameter of 0.58 mm and an outer diameter of 1.0 mm, and they are collectively fused in a circular pattern with an equivalent outer diameter

Table 2 The samples of microfluidics preparation of NDDSs.

NDDS	Microfluidic device	Control condition	The feature of NDDSs				Ref.
			Size (nm)	Dispersion	Shape	Others	
Liposomes	Hydrodynamic flow focusing	Flow rates; Concentrations	50–110	<0.2	Spherical	Enhanced cell uptake	59
Doxorubicin-loaded lipid-based NDDSs	Microfluidic mixer chip	FRR; TFR	92–269	<0.2	Spherical	Have better tumor regression and overall survival rates	60
Curcumin-loaded liposomes	Staggered herringbone micromixer	TFR; FRR; drug-to-total lipid ratio	120	<0.2	Spherical	Augmented the antitumor efficacy and decreased the nephrotoxicity	61
Multi-responsive liposomes	Microfluidic mixer chip	FRR; TFR	60–110	<0.2	Spherical	–	62
Niosome nanoparticles	Microfluidic mixer chip	–	158	<0.2	Spherical	Raise high antibody immune responses	56
Liposomes	Microfluidic mixer chip	The average flow velocity; TFR; aspect-ratio of microfluidic device	80–120	<0.2	Spherical	–	63
Liposomes	Microfluidic hydrodynamic focusing device	Flow rates	40–120	Excellent	Spherical	High drug-loading efficiency	64
Liposomes	Staggered herringbone chaotic micromixer	Flow rates	50–150	Excellent	Spherical	–	65
LNPs	Staggered herringbone micromixer	Flow rates; Concentrations	20–55	<0.03	Spherical	Highly efficient delivery of siRNA	66
LNPs	Y-shape staggered herringbone micromixer	FRR; TFR	80–100	<0.25	Spherical	Highly efficient delivery of siRNA	67
LNPs	Staggered herringbone micromixer	The channel of parallel microfluidic device	<30	Excellent	Spherical	Highly efficient delivery of mRNA and siRNA	68
Solid LNPs	Glass capillary-based microfluidic-chip	Flow rate	100–200	0.16–0.23	–	Highly efficient delivery of PTX and SLNs	69
LNPs	iLiNP device	Flow rate; Concentrations of lipid	80–150	0.08–0.18	Spherical	Highly efficient delivery of siRNA	70
Cabazitaxel-loading albumin nanoparticles by microfluidics (MF-CTX-NPs)	Microfluidics chip	Flow ratio; Concentrations	142.1 ± 2.7	0.095	Spherical	Enhanced tumor uptake; increased the therapeutic efficacy	49
Folic acid-modified MF-CTX-NPs (FA-MF-CTX-NPs)	Microfluidics chip	Flow ratio	162.4 ± 3.1	0.102	Spherical	Increased delivery efficiency of CTX; strong tumor inhibition	71
BCA-P ₁₁₄ nanoparticle	Acoustically actuated microfluidic mixer	Concentrations of MgCl ₂ ; Mixing time and strength	207.5	1	Spherical	–	72
Bovine serum albumin nanoparticles	Microfluidics chip	Flow ratio; Concentrations	122.5 ± 0.9	0.107	Spherical	Increases drugs solubility; decreases drug cytotoxicity	73
Pea protein-curcumin nanoparticles	Microfluidics chip	Pressure; Concentrations	271.3	0.16–0.53	–	Increases drugs solubility	74
DOX@ZIF-8@SiO ₂ nanoparticles	T-junction thermal-assisted microfluidic system	The type of chip	67.7 ± 22.1	–	Spherical	High tumor inhibition	75
pCas9pPXN@NPs@PDDA	Microfluidics chip	Concentration of NPs and polymer; FRR	–	–	Spherical	Improve the nuclear plasmid delivery efficiency	76
TMC/Pd nanoparticles	Microfluidics chip	Flow rate; FRR	84.4 ± 33.8	–	Spherical	Enhanced biocompatibility	77

(continued on next page)

Table 2 (continued)

NDDS	Microfluidic device	Control condition	The feature of NDDSs			Ref.	
			Size (nm)	Dispersion	Shape		
DPSi/DaU@AcDEX nanoparticles	Microfluidics chip	—	473 ± 13	0.19	Spherical	Effectively loads the drugs; identify pathological changes in the tissues	78
mPEG- <i>b</i> -p(HPMA- <i>Bz</i>) micelles	A commercial herringbone micromixer glass chip	Flow rates; Concentrations	35–90	Excellent	Tune	—	79
p(HPMAm)- <i>b</i> -p(HPMAm- <i>Bz</i>) micelles	Microfluidics chip	Flow rates; Concentrations	40–120	Excellent	—	—	80
Docetaxel micelles	Microfluidics chip	Concentrations of PLGA	72	0.072	Spherical core-shell structure	Highly efficient delivery of chemotherapeutic drugs for cancer treatment	81
Paclitaxel micelle	Hydrodynamic flow focusing device with herringbone mixer	The variation of the drug; polymer ratio	90; 180	~0.2	Spherical	Enhanced cytotoxic activity; better tumor cell internalization	82
Block copolymer micelles	An interdigital passive micromixer	Flow ratio	30 ± 6	0.17	Spherical	—	83
Shellac polymer nanoparticles	2D microfluidic devices	Flow rates	40–100	0.1–0.4	Spherical	High encapsulation efficiency of drugs	84
PNPs	Microfluidic chips	Flow rates	50–150	0.1–0.3	Spherical	—	85
SN-38-PNPs	Microfluidic chips	Flow rates	100–1000	—	Spherical	High encapsulation of SN-38	86

—, not applicable; NDDSs, nano-drug delivery systems; FRR, flow rate ratio; TFR, total flow rate; PNPs, polymer nanoparticles; LNPs, lipid nanoparticles.

of 3 mm (as shown in Fig. 6A⁴³). LNPs synthesized by this 3D-HFF device presented unprecedentedly low levels of polydispersity. The evaluation of the flow FRR effect on LNPs further indicated that higher FRR decreased PDI.

The dilution efficiency of lipid solution is also another important parameter to control the physicochemical properties of LNPs¹³⁰. A higher dilution efficiency of lipid solution can result in a narrower size distribution of NDDSs¹³¹. In order to improve the dilution efficiency, many researchers are devoted to developing microfluidic devices with chaotic mixer^{132,133}. Chaotic advection in the microchannels can be generated by local rotational and extensional flows, thus the dilution efficiency of lipid solution is rapidly enhanced³⁴. Our group prepared Tf-LNPs by a 3-inlet microfluidic device with herringbone structure and S-type channels, and the scheme is presented in Fig. 6B⁴⁸. In this work, we compared the microfluidic method with a multi-step bulk mixing method for synthesizing Tf-LNPs. The results indicated that microfluidics enables a rapid and efficient synthesis of Tf-LNPs. Compared with Tf-LNPs produced by the multi-step bulk mixing method, Tf-LNPs prepared by microfluidics had a smaller size and more uniform structures. Moreover, because the herringbone structure and S-type channels can excellently improve the mixing efficiency between lipid solution and siRNA solution, Tf-LNPs prepared by microfluidics showed more efficient cellular uptake *in vitro*, greater tumor inhibition, and higher siRNA delivery efficiency *in vivo*. Moreover, the appropriate cycle number or deeper micromixer structures lead to a higher mixing efficiency^{51,52}. Maeki et al.⁵⁰ fabricated microfluidic devices with chaotic micromixers possessing different cycle numbers (0, 2, 6, 10, 20, and 69 cycles). The LNPs sizes were found to range from 40 to 150 nm. LNPs produced by microfluidic devices with 10, 29, and 69 cycles produced LNPs that were smaller and less dispersed. Meanwhile, deeper chaotic micromixers were found to have higher mixing performance than that of shallower ones.

Although the microfluidic devices with chaotic mixers improved mixing efficiency between reagents, a clogged problem still exists^{36,42}. In order to overcome this limitation, Kimura et al.⁴² developed the two-dimensional baffle mixer device (named as iLiNP device) for producing LNPs (as shown in Fig. 6C⁴²). iLiNP device with a baffle mixer (width of 150 μm, depth of 100 μm, and interval of 100 μm) was fabricated by standard photolithography. The baffle mixer is similar to a zigzag-shaped microchannel and its microchannel has a width of 200 μm and a height of 100 μm. In their work, LNPs were prepared by iLiNP and microfluidic device with chaotic mixer, respectively. Results indicated that iLiNP has higher mixing efficiency than the chaotic mixer device at high flow rate conditions and the clogging problem was well solved. Meanwhile, the dimensions of the baffle structure, such as width and depth, showed an important effect on controlling the size of LNPs.

3.2.2. Polymer nanoparticles

PNPs usually include polymer nanospheres and nanocapsules¹³⁴. Among them, polymer nanospheres are matrix particles, which can be used as carriers for bioactive molecules including drugs¹³⁵, genes¹³⁶, nucleic acids¹³⁷, fluorescence¹³⁸, and other functional substances¹³⁹. Unlike polymer nanospheres, polymer nanocapsules are vesicle systems in which the bioactive agents are confined within a water core and surrounded by a polymer shell¹³⁴. The surface of polymer nanoparticles can be functionalized by coupling a series of metal ions, small molecules, and surfactants to achieve drug targeting and avoid immune

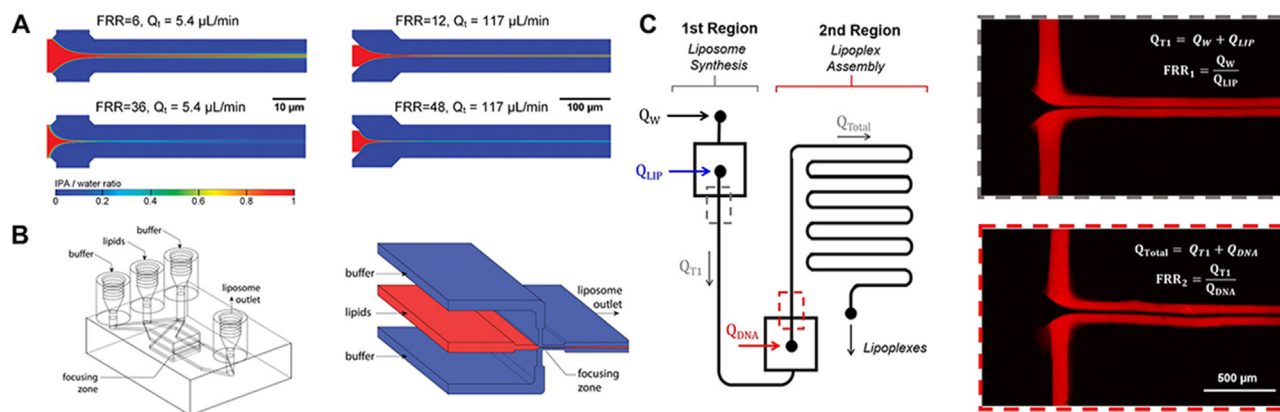


Figure 5 (A) Numerical simulations of microfluidic device design and HFF (Reprinted with the permission from Ref. 96. Copyright © 2010 American Chemical Society). Mixing and surface-to-volume ratio of the focused IPA stream in both channel geometries increases with the increase of FRR. A higher FRR could produce smaller-sized liposomes with narrow size distribution. (B) Vertical flow focusing chip model, and magnified schematic of the focusing region (Reprinted with the permission from Ref. 98. Copyright © 2019 WILEY-VCH). High-throughput preparation of liposomes can be achieved by this technique with their productivity up to 4 mg/min. (C) Schematic representation of the microfluidic devices for the one-step formation of plasmid DNA (pDNA)/CL lipoplexes (Reprinted with the permission from Ref. 99. Copyright © 2017 Elsevier B.V.).

response¹⁴⁰. As a drug delivery system, polymer nanoparticles have the following advantages: 1) high drug-loading capacity¹⁴¹; 2) high cellular uptake efficiency¹⁴²; and 3) good stability and biocompatibility¹⁴³. At present, their synthesis methods include solvent rotary evaporation¹⁴⁴, emulsification solvent diffusion¹⁴⁵, and solvent displacement¹⁴⁶, etc. However, polymer nanoparticles obtained by these methods have some common problems, such as large particle diameter, broad particle size distribution and poor continuous synthesis ability¹⁴⁷.

In order to obtain PNPs with smaller particle size, narrower size distribution, high drug-loading capacity, and better repeatability, many researchers have applied microfluidic technology¹⁴⁸. During the formation of PNPs, processes such as mixing, droplet generation, and nano-precipitation can be precisely controlled, which cannot be achieved by traditional methods. The most commonly used microfluidics device for synthesizing PNPs is microfluidic focusing device¹⁴⁹. The principle is microfluidic nano deposition that the low solubility of the polymer in the aqueous

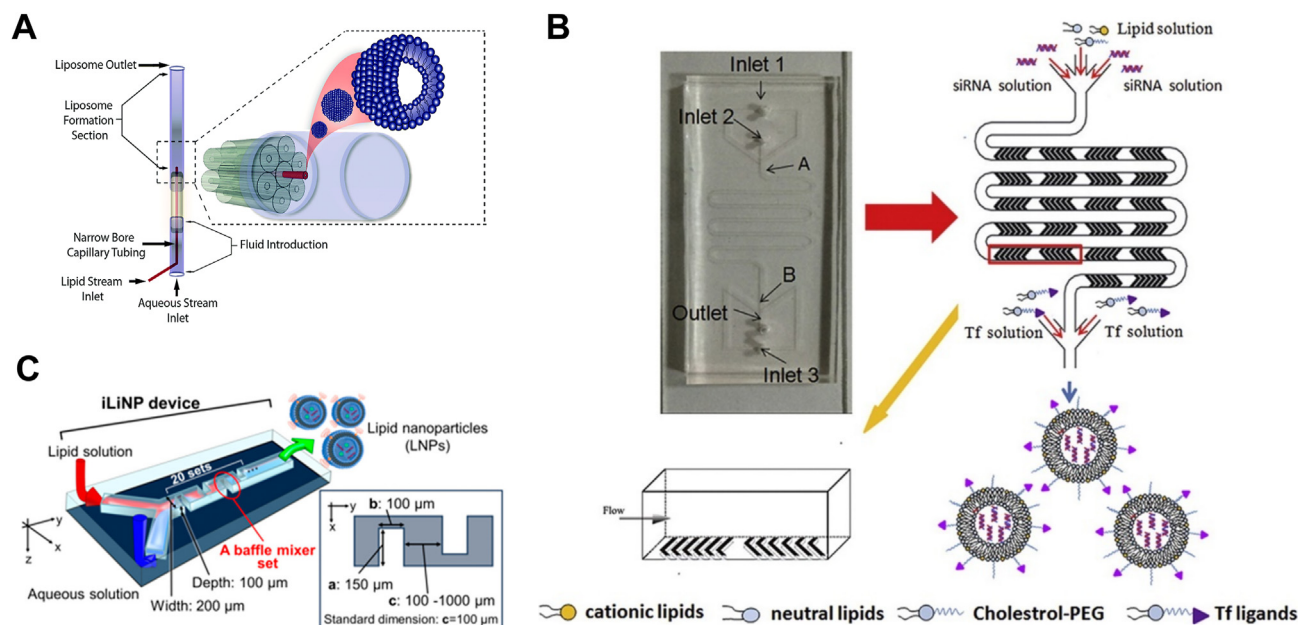


Figure 6 (A) 3D-HFF microfluidic device with seven identical borosilicate glass capillaries in a large capillary for fabricating LNPs (Reprinted with the permission from Ref. 43. Copyright © The Royal Society of Chemistry 2014). Each capillary possesses an inner diameter of 0.58 mm and an outer diameter of 1.0 mm, and they are collectively fused in a circular pattern with an equivalent outer diameter of 3 mm. (B) Schematic of Tf-LNPs by microfluidic device with herringbone structure and S-type channels (Reprinted with the permission from Ref. 48. Copyright © 2016 Elsevier Inc.). (C) iLiNP possessing a microchannel with a width of 200 μm and a height of 100 μm for fabricating LNPs (Reprinted with the permission from Ref. 42. Copyright © 2018 American Chemical Society).

phase leads to the precipitation of polymer in the water/organic interface, followed by the formation of PNPs¹⁵⁰. Martín-Banderas et al.¹⁵¹ prepared PNPs loaded with gemcitabine by microfluidics. They found that drug encapsulation efficiency was twice than that of the solvent rotary evaporation method and the drug sustained-release effect was better. Meanwhile, they also presented an improved antitumor effect. Baby et al.⁸⁴ also reported a novel microfluidic nanocrystalline precipitation technique for the preparation of polymeric nanoparticles with a drug loading of up to 50%, and the drugs' release can be adjusted efficiently by changing pH. In this way, the tunable drug-loading capacity and the controllable drug release of PNPs were successfully achieved. Results showed that the particle size of PNPs is significantly correlated to their biological functions¹⁵². Gimondi et al.¹⁵³ investigated the effect of several parameters (*e.g.*, polymer concentration, flow rate, and FRR between aqueous and organic solutions) on the physicochemical properties of PNPs, and confirmed that the particle size of PNPs strongly affects their drug encapsulation, delivery ability, and other biological functions.

As one of the most widely used degradable polymer organic compounds, PLGA has the advantages of good biocompatibility, non-toxicity, and easy degradation, etc¹⁵⁴. PLGA PNPs obtained by microfluidics have great application prospects in drug delivery¹⁵⁵. Karnik et al.¹⁵⁶ prepared PNPs by different methods, including

microfluidics and solvent rotary evaporation method, and the schematic diagram is shown in Fig. 7A¹⁵⁶. They found that the particle size of the microfluidic-generated PLGA PNPs was 34 nm, while the particle size of the PLGA PNPs synthesized by solvent rotary evaporation method was 105 nm. They proved that PNPs prepared by microfluidics are much smaller in size than those obtained by traditional method. In order to study how to obtain PNPs with smaller sizes by changing the experimental conditions, Leung et al.¹⁵⁷ used microfluidic hydrodynamic focusing to load curcumin into PLGA PNPs and found that flow rate and FRR played an important role in particle size, PDI and encapsulation efficiency of PLGA nanoparticles. Similarly, the preparation of PLGA PNPs by microfluidics can also be used to deliver other drugs, such as nucleic acid drugs. Zoqlam et al.¹⁵⁸ prepared PLGA-Eudragit nanoparticles encapsulating plasmid DNA by microfluidics (as shown in Fig. 7B¹⁵⁸). Compared with PLGA-Eudragit nanoparticles obtained by traditional methods, DNA transfection efficiency of microfluidic-prepared PLGA-Eudragit nanoparticles was higher. However, PLGA can easily clog microchannels owing to their large molecular weight, thus limiting their clinical mass production¹⁵⁹. To overcome this shortcoming, Liu et al.¹⁶⁰ designed a 3D coaxial flow microfluidic device to prepare PNPs. This device inserts a conical glass capillary into another larger cylindrical capillary and aligns it coaxially. The inner fluid (4% ethanol solution containing

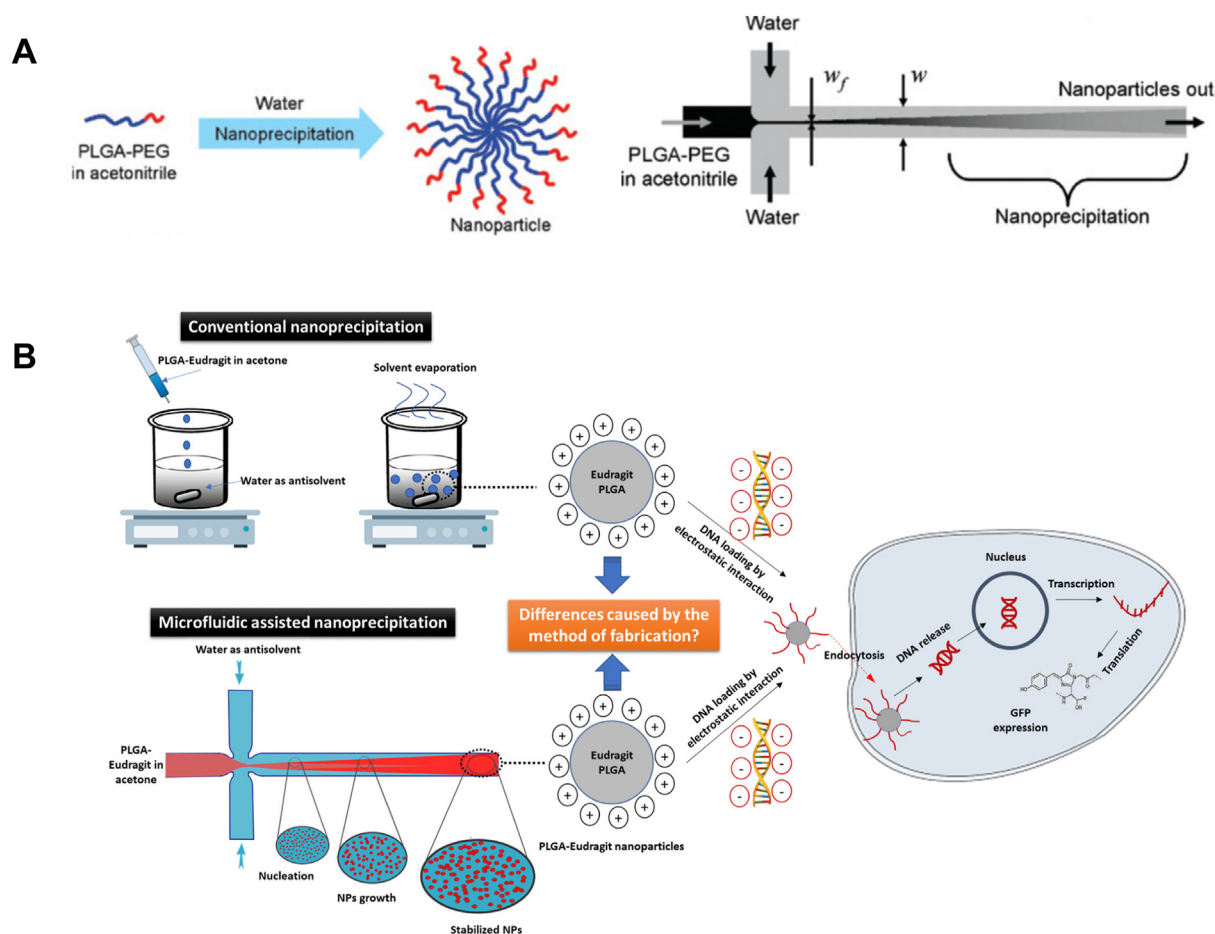


Figure 7 (A) The schematic diagram of prepared PNPs by microfluidics. The process of mixing in a microfluidic device using HFF (Reprinted with the permission from Ref. 156; Copyright © 2008 American Chemical Society). (B) The fabricating process of PLGA-based nanoparticles by microfluidics (Reprinted with the permission from Ref. 158; Copyright © 2021 Elsevier B.V.).

50 µg/mL phospholipids as a stabilizer) flows inside the inner cylindrical capillary, while the outer fluid (50 mg/mL PLGA acetonitrile solution) flows between the inner and outer cylindrical capillaries. The use of this microfluidic platform not only solves the problem that PLGA is easy to block the channel, but also ensures that the prepared nanoparticles have a uniform size distribution, and the particle size and surface charge can also be easily adjusted, thereby providing a potential method for clinical large-scale production.

3.2.3. Protein nanoparticles

Protein nanoparticles-based NDDSs are formulations in that drugs are encapsulated into protein nanoparticles¹⁶¹. Drugs can be covalently bound in the three-dimensional spatial structure of the protein or doped in the matrix, which can protect drug molecules from degradation^{162,163}. Protein nanoparticles, as a drug carrier, have been widely applied in drug delivery owing to their excellent properties such as low toxicity, good biocompatibility, high biodegradability, and high affinity^{164–166}. Owing to the excellent property of microfluidics, it has also been used to fabricate protein nanoparticles⁵⁰. In the microfluidic system, aqueous and organic phases are simultaneously injected into a microfluidic chip by a high-pressure delivery pump. The liquid experiences turbulent flow, laminar flow, or atomization in the microfluidic chip, and two-phase mixing is realized³⁵. Under the action of the high-pressure delivery pump, the particle size of protein nanoparticles can be reduced by impact force and shear force, thereby achieving a stable and controllable continuous synthesis of homogeneous protein nanoparticles^{56,167}.

Jeon et al.¹⁶⁸ prepared protein nanoparticles by continuous-flow microfluidics. In their work, Ni-NTA-PS solution was introduced into the central inlet channel at a flow rate of 40 µL/min, while His-GFP PBS buffer was introduced into both sides of the inlet at a flow rate of 20 µL/min. The Re of the obtained His-GFP solution was 3.45, and the Re of the polymer solution was 6.87, indicating that the flow was in a strong laminar state. To solve the blockage of protein nanoparticles, they added a delayed entry channel and introduced a DMF solution to avoid the direct contact of Ni-NTA-PS with His-GFP solution. However, the formation of protein nanoparticles could be easily disrupted in a microfluidic system, because proteins and small molecules are easily absorbed by PDMS materials¹⁶⁹. In order to overcome this limitation, Jeon et al. modified the surface properties of transparent glass slides and PDMS molds with oxygen plasma, and hydrophobically modified channel surfaces using liquid-phase evaporated dichloro dimethyl silane self-assembled monolayers¹⁶⁸.

Since the microfluidic chip can precisely control liquid mixing and maintain a high mixing efficiency, protein nanoparticles-based NDDSs with a higher encapsulation efficiency can be obtained. In order to improve the drugs' encapsulation efficiency, our group designed an inverted W-type microfluidic chip by conventional UV photolithographic and soft-lithography for preparing CTX-NPs⁴⁹. Human serum albumin containing sufficient drug binding sites was used as protein material, and microfluidic technology and traditional method were used to prepare protein nanoparticles, respectively. The results indicated that obtained MF-CTX-NPs have a higher drug-loading capacity and encapsulation efficiency than CTX-NPs fabricated by the traditional method (BU-CTX-NPs). Besides, MF-CTX-NPs exhibited more uniform and narrower particle size and dispersion. MF-CTX-NPs also showed better tumor inhibition *in vivo*, which can be attributed to the improved mixing efficiency between the outer aqueous phase and

the internal organic phase⁴⁹. To improve the targeting of MF-CTX-NPs, we fabricated FA-MF-CTX-NPs, and the scheme is presented in Fig. 8A⁷¹. Compared with MF-CTX-NPs, FA-MF-CTX-NPs enhanced tumor targeting and exhibited more pronounced tumor suppressive effects, both *in vitro* and *in vivo*. Meanwhile, FA-MF-CTX-NPs also prolonged the blood circulation time. Different from the albumin self-assembly method employed by our group, Hakala et al.¹⁷⁰ developed a 3D co-flow device to generate protein nanoparticles by co-flowing an aqueous protein solution and celastrol ethanol solution. In their design, a water flow was added into the outer layer. The addition of the water flow squeezed ethanol and protein, making the two phases diffuse rapidly. In addition, water layer also hinders the direct contact of proteins with PDMS and reduce their adhesion. The nanoparticles obtained by 3D co-flow device are stabilized by intermolecular disulfide bonds, thereby eliminating the need for toxic crosslinkers¹⁷¹. This 3D co-flow device increased the encapsulation efficiency of celastrol in protein nanoparticles, and significantly reduced its cytotoxicity.

Recently, more microfluidic devices have been designed for the preparation of protein nanoparticles¹⁷². Acoustically driven microfluidic mixers are designed to solve the problem of prolonged mixing between reagents⁶⁴. It can homogenize nanoparticles within 6 ms and can mix reaction solution efficiently and quickly to prevent concentration fluctuations and minimize particle size variation of protein nanoparticles⁶⁴. Furthermore, an electrodynamic-based fast-mixing microfluidic device was developed, which can generate turbulent-like flow under the action of an alternating electric field to assemble functional proteins and polymers in an ethanol/water co-solvent system. The physicochemical properties of protein nanoparticles can be easily controlled and tuned by adjusting the alternating current electric field (*e.g.*, voltage, frequency, signal phase shift) and flow rate, which also provide a new strategy to obtain protein nanoparticles⁷³.

3.2.4. Inorganic nanoparticles

Compared with organic nanoparticles, inorganic nanoparticles, such as silica nanoparticles^{173–175}, metal nanoparticles^{176–178} and quantum dots¹⁷⁹, show better mechanical and chemical stability¹⁸⁰. Moreover, many inorganic nanoparticles also have special optical photothermal and magnetic properties^{181–183}. Therefore, inorganic nanomaterials have attracted extensive attention in drug delivery^{184,185}. However, the nanoparticles obtained by traditional preparation methods have poor stability and uncontrollable particle size, which limit their clinical translation¹⁸⁶. Microfluidics had been widely applied to controllably prepare inorganic nanoparticles owing to its unique properties. The principle of preparing nanoparticles by microfluidics is similar to traditional methods. The fabrication of inorganic nanoparticles mainly consists of two steps¹⁸⁷. The first step is the nucleation stage, in which the supersaturated inorganic salt solution is deposited into an insoluble monomer and then assembled into small nanoparticles, and the second step is the growth stage during which the tiny inorganic nanoparticles grows¹⁸⁷. It is generally believed that the nucleation and growth happened simultaneously throughout the formation of NDDSs. A higher nucleation rate and a slower growth rate can obtain stable and ultrafine NDDSs with a small distribution coefficient⁵³. The high mixing efficiency is helpful in creating high nucleation rates, and smaller and more uniform NDDSs with higher drug-loading capacity can be obtained^{53,188}. Different from the principle of the nano-precipitation method for organic nanoparticles, microfluidic preparation of inorganic nanoparticles

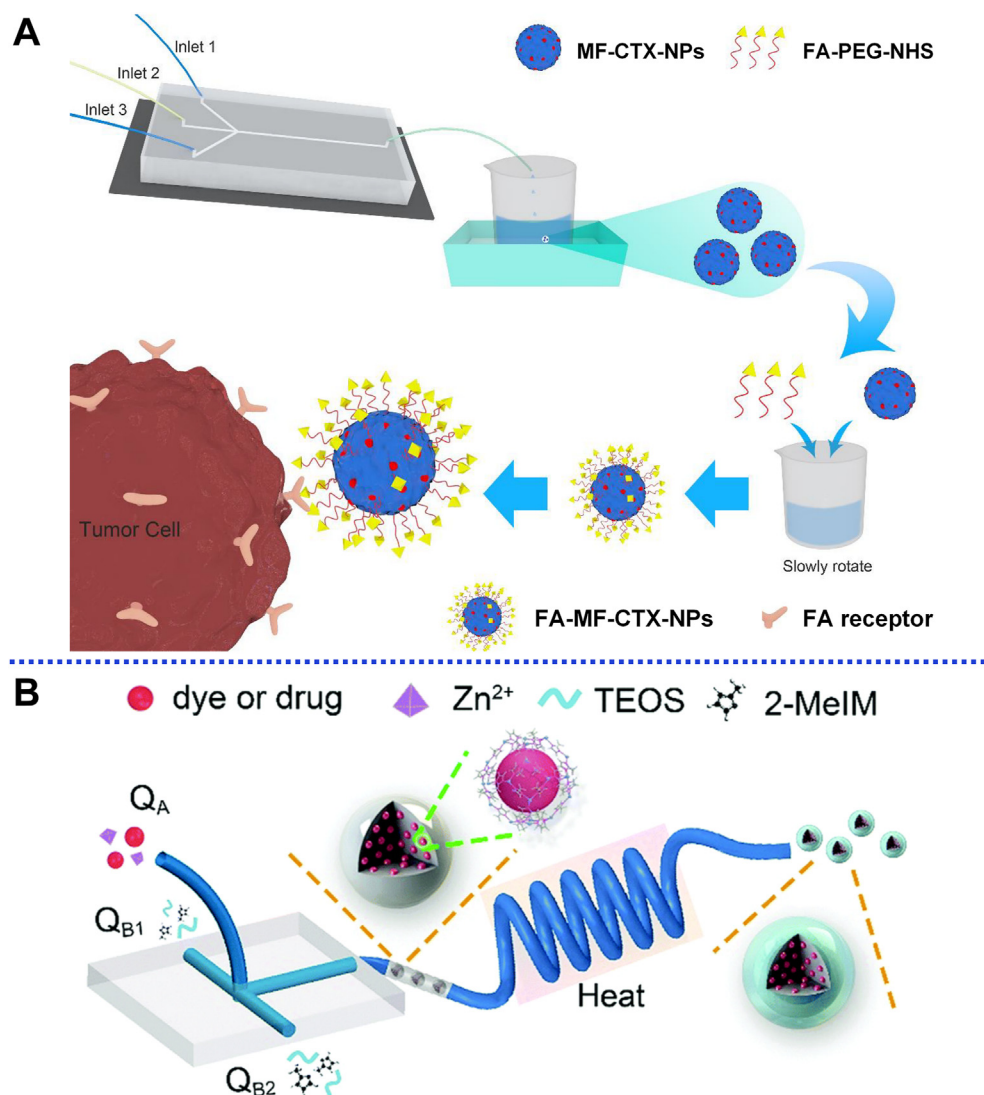


Figure 8 (A) Schematic illustrations of the preparation of FA-MF-CTX-NPs by inverted W-type microfluidic chip (Reprinted with the permission from Ref. 71; Copyright © 2019 by the authors). FA-MF-CTX-NPs enhanced tumor targeting and exhibited more pronounced tumor suppressive effects, both *in vitro* and *in vivo*. (B) Schematic illustration of the microfluidic system for the synthesis of drug@ZIF-8@SiO₂ (Reprinted with the permission from Ref. 75; Copyright © The Royal Society of Chemistry 2018).

usually involves a chemical reaction, which requires reagent addition, separation, and purification¹⁶. The size distribution and shape of nanoparticles can be adjusted by adjusting pH, saturation degree of solution, and flow rate of liquid^{189–191}.

Silica nanoparticles with a large specific surface area, strong loading capacity, good biocompatibility, and surface modification are suitable for biomedical field¹⁸³. Continuously flowing microfluidics and segmented-flow microfluidics have all been widely applied to synthesize silica nanoparticles^{192,193}. In 2004, Khan et al.¹⁹⁴ designed a continuous-flowing microfluidic device with two inlets leading to a mixing channel to fabricate silica nanoparticles for drug delivery, and the effect of flow rates for silica nanoparticles was investigated. In this work, ethyl orthosilicate as silica precursor was diluted by ethanol solution. Then, ammonia and ethanol solution were pumped into the microfluidic device, respectively. The results indicated that silica nanoparticles with an average diameter of 321 nm and a size deviation of 9% were obtained at low flow rates. At high flow rates, smaller silica

nanoparticles (164 nm) were obtained in 3 min, but their size deviation was significantly increased by 25% due to axial dispersion of colloidal particles. In order to overcome this drawback, they then used a segmented flow device to eliminate this axial dispersion effect¹⁹⁴. Later, He et al.¹⁹⁵ constructed two microfluidic devices including a single-phase continuous-flow microreactor (CFMR) and a two-phase segmented-flow microreactor (SFMR). This device can minimize the effect of particle deposition in the reaction tube while maintaining constant flow conditions. Similarly, tetramethoxy silane was used as a silicon source, and PEI was used as a nucleation catalyst, and silica nanoparticles with a diameter less than 100 nm were prepared. The yield is higher than that of batch synthesis. The size and size distribution can be easily adjusted by changing pH, flow rate, and residence time. Since the axial dispersion effect is eliminated under SFMR conditions, the size distribution of silica nanoparticles is narrower than that of CFMR¹⁹⁵. However, microfluidics can not only be used to fabricate silica nanoparticles but

also to coat other materials such as polymer layers on the surface of silica nanoparticles^{196–198}. Polymer layers can be used as a response layer to protect the bioactivity and control the release of drugs¹⁹⁸. Yan et al.¹⁹⁹ fabricated a pH/redox-triggered MSN nanoplatfoms for co-delivery of DOX/PTX by a microfluidic device. First, PTX was covalently attached to the surface of DOX-loaded MSN *via* disulfide bonds, and then, PSS was electrostatically adsorbed on DOX@MSN-PTX in a microfluidic device, which can effectively protect the activity of PTX and DOX. Under acidic conditions, MSN-NH₂ is protonated, and the electrostatic interaction is disrupted at pH = 5. The covalent binding sites as redox-sensitive switches can precisely control the release of DOX and PTX, and thus DOX@MSN-PTX@PSS can be pH/redox-triggered. *In vitro* experiments proved that DOX@MSN-PTX@PSS could effectively and selectively kill BT549 cancer cells and had no effect on healthy breast cells MCF-10A¹⁹⁹. Similarly, Xu et al.⁷⁶ prepared functionalized MSNs with high loading efficiency to deliver CRISPR/Cas9 plasmids, and then adsorbed PDDA on the surface of MSNs, thus effectively preventing EcoRV restriction endonuclease enzyme-induced degradation of the plasmid to promote nuclear translocation. Kucukturkmen et al.²⁰⁰ also used a microfluidic device to encapsulate PDDA in an outer layer of monodisperse silica nanoparticles to maintain the biological activity of the internally encapsulated protein. The use of this microfluidic device for secondary modification of MSNs and the modification of pH-sensitive polymer (arginine-modified acetyl dextran) on the surface of silica nanoparticles can further improve the stability of the protein and prevent their premature release.

In addition, metal nanoparticles, because of their unique optical, mechanical, chemical, and catalytic properties, have been widely used in biomedical fields¹⁸⁷. Precious metal nanoparticles (*e.g.*, Au and Ag) is also a promising drug delivery carrier due to their excellent biocompatibility and easy to combine with a variety of biological molecules such as target ligands¹⁶. Continuously flowing microfluidics had been widely applied to synthesize metal nanoparticles-based NDDSs^{201,202}. Hao et al.²⁰³ designed a microfluidic device with a micro-spiral-shaped double inlet, and core-silicon-shell nanoparticles (Ag@SiO₂) with adjustable silicon shell thickness was synthesized by this continuously-flowing microfluidics. Zhang et al.²⁰⁴ developed a simple, fast, and feasible temperature-programmed microfluidic process, combined with surface modification and functionalization of nanohybrids, to prepare nanomedicines with multimodal imaging capabilities and good antitumor effects (*e.g.*, Au@CoFeB-Rg3). Au@CoFeB-Rg3 had obvious inhibitory effects on human hepatoma cells (HepG2/C3) and human chronic myeloid leukemia cells (K562), and it was found that the hybrid nanoparticles had an obvious synergistic effect with Rg3. Additionally, the CoFeB shell was superparamagnetic and strongly interacted with X-ray radiation, which could be tracked by MRI and CT imaging, thus making the drug more accurate and visible *in vitro* and *in vivo*, and further facilitating clinical application.

MOFs have also attracted researchers' extensive attention due to their unique advantages such as large surface area²⁰⁵, high porosity, and biodegradability²⁰⁶. Hu et al.⁷⁵ developed a thermally-assisted microfluidic system consisting of a T-shaped PDMS core and PTFE tube attachments for continuous and scalable preparation of drug-loaded MOFs@SiO₂ nanoparticles, the scheme is shown in Fig. 8B⁷⁵. Rose Bengal photosensitizer (RB) and DOX were successfully encapsulated into the nanoparticles, which showed great potential in tumor therapy and photodynamic

therapy⁷⁵. Moreover, MOFs are also used for insulin delivery. Rohra et al.²⁰⁷ reported the microfluidic synthesis of MOFs in response to glucose stimulation. They synthesized ZIF-8 loaded with insulin and gold nanoparticles (AuNPs) *via* a continuous-flow microfluidic mixing system, which increased the insulin loading capacity to 77%–88%. Drug release studies confirmed the response of MOFs to glucose to trigger insulin release²⁰⁷.

4. The industrialization and challenges of microfluidics-mediated NDDSs

As aforementioned, microfluidics-mediated NDDSs have achieved outstanding research results in laboratory studies due to their diverse compositions, precise size control capabilities, and ease of production^{2,32}. To date, with the rapid development of scientific research and industrial technologies, microfluidics-mediated NDDSs have been promoted and applied in industrial processes to meet the growing needs of human life and production. For instance, in 2018, the first small interfering RNA (siRNA)-based drug patisiran, namely Onpatro®, developed by Alnylam Pharmaceuticals and Sanofi-Aventis, was approved by the U.S. Food and Drug Administration (FDA) for the treatment of adults that suffered from polyneuropathy triggered by hATTR, which paved a way for the fabrication of microfluidics-mediated NDDSs towards industrialization²⁰⁸. Recently, although many microfluidics-mediated NDDSs have been reported for some disease therapy including genetic diseases and cancer, there is still a small step away from large-scale industrialization. Since 2019, with the rapid spread of COVID-19 to more than 200 countries, which caused severe economic consequences and huge loss of lives. The emergence of the COVID-19 vaccine greatly stimulated the development and application process of microfluidics-mediated NDDSs, thereby accelerating microfluidics-mediated NDDSs for more than 30 years in laboratory research to industrial production.

At present, the marketed microfluidics-mediated NDDSs against COVID-19 include Pfizer/BioNTech's BNT162b2 and Moderna's mRNA-1273, both of which are LNPs-encapsulated mRNA vaccines^{16,33}. In these two commercial products, LNPs are used as drug carriers, which have the advantages of easy formulation, good biocompatibility, large loading capacity, and protecting mRNA from degradation. They are composed of cationic lipids, cholesterol, helper lipids, and PEG lipids, and are till now the only mRNA delivery carrier approved by the FDA for industrial production (search on [fda.gov](https://www.fda.gov)). In the preparation of LNPs, ionizable lipids can associate with mRNA molecules through electrostatic interactions under acidic conditions to form nanoparticles, deliver mRNA into cells *via* endocytosis, and also enhance mRNA escape from endosomes. We summarize relevant information on commercial microfluidics-mediated NDDSs, as presented in Table 3.

Pfizer uses an IJM to produce mRNA-loaded LNPs. The physical picture of IJM device which is used in laboratory and industrialization are shown in Fig. 9A and B, respectively. IJM device used by Pfizer was obtained from KNAUER company (Germany) and was configured with up to eight parallel mixing units. Unlike the devised used in the laboratory, the device accessories are simplified and each unit consists of two pumps (lipid pump, API pump), two flow meters and one jet mixer in industrialization. In which, the pump was used to deliver lipid and active pharmaceutical ingredient solution, and flow rate was controlled by flow meter. The relevant parameters of IJM device

Table 3 The relevant information on FDA-approved microfluidics-mediated NDDSs, search on fda.gov.

Product name	Patisiran	BNT162b2	mRNA-1273
Market time	2018	2021	2021
Company	Alnylam/Sanofi-Aventis	Pfizer/BioNTech	Moderna
Type	siRNA drug	mRNA vaccine	mRNA vaccine
Drug	siRNA silencing hATTR	Nucleoside-modified mRNA encoding viral spike (S) glycoprotein of COVID-19	Nucleoside-modified mRNA encoding viral spike (S) glycoprotein of COVID-19
Indication	Adults with polyneuropathy caused by hATTR	COVID-19	COVID-19
Mechanism	hATTR mRNA silence	Immune response	Immune response
Microfluidic device	Undisclosed	Impingement jet mixer	Undisclosed
Cationic lipid	DLin-MC3-DMA	ALC-0315: (4-hydroxybutyl) azanediy)bis(hexane-6,1-diyl)bis(2-hexyldecanoate)	SM-102: heptadecan-9-yl-8-((2-hydroxyethyl) (6-oxo-6-(undecyloxy)hexyl) amino) octanoate
PEG-lipid	PEG2000-C-DMG: 1,2-dimyristoyl- <i>rac</i> -glycero-3-carboxylaminoethyl- ω -methoxypolyethylene glycol-2000	ALC-0159: 2-[(polyethylene glycol)-2000]- <i>N,N</i> -ditetradecylacetamide	PEG2000-DMG: 1,2-dimyristoyl- <i>rac</i> -glycero-3-methoxypolyethylene glycol-2000
Helper lipid	DSPC	DSPC	DSPC
Cholesterol	Cholesterol	Cholesterol	Cholesterol
Others	Monobasic potassium phosphate Sodium chloride Sodium phosphate dibasic Heptahydrate —	Monobasic potassium phosphate Sodium chloride Sodium phosphate dihydrate dibasic Potassium chloride, sucrose	Tromethamine hydrochloride Acetic acid Sodium acetate Tromethamine, sucrose

COVID-19, coronavirus disease 2019; hATTR, hereditary transthyretin-related amyloidosis; PEG, polyethylene glycol.

used in industrialization are presented in Table 4. Briefly, the lipid solution was pumped on one side and mRNA was pumped on the other, and they were mixed together with pressure of 400 pounds. The mixture was then quenched in a third mixer where the high mixing velocity could reduce the solubility of the lipids so that homogenous mRNA-loaded LNPs could be formed. To improve the production efficiency of BNT162b2 vaccine, Pfizer achieved a parallelization of multiple static mixers by replicating the quarter-

sized mixers, which allow the continuous synthesis and the increase of their vaccine productivity at the Kalamazoo (US) site to 100 million doses per month²⁰⁹. However, till now, the microfluidic device for Moderna's mRNA-1273 has not been disclosed though it was used for vaccine production.

In China, there are also some companies that use microfluidic technology to prepare microfluidic-based NDDSs. For instance, StemRNA Therapeutics Co., Ltd. and micro&nano Biologics Co.,

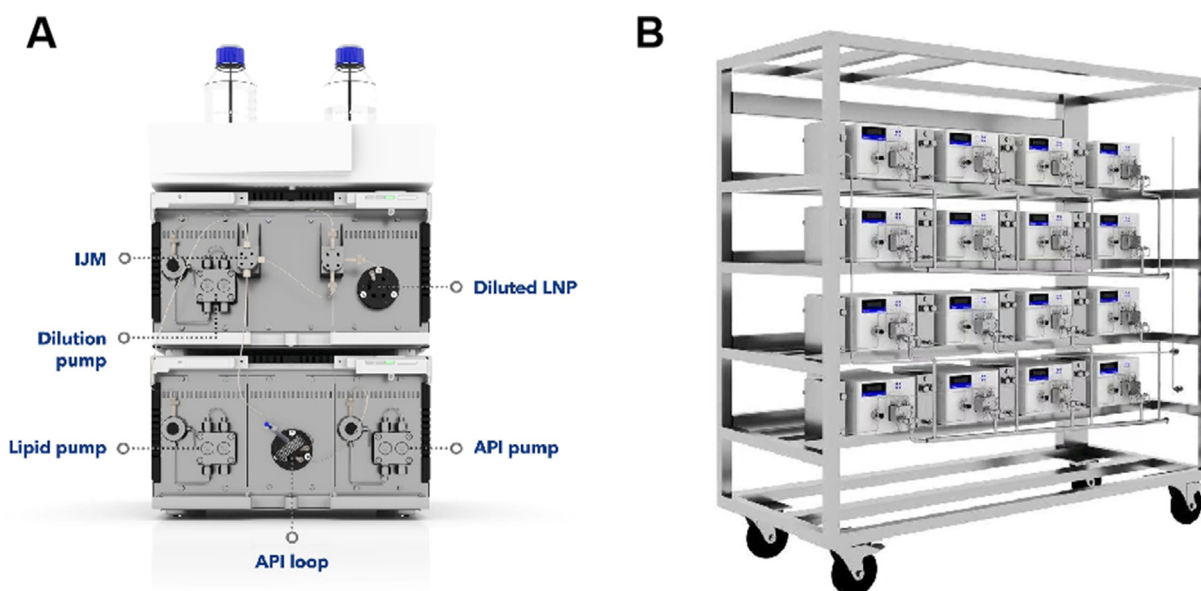


Figure 9 The physical pictures of IJM device which is used in laboratory (A) and industrialization (B). The figures were provided by Lumiere Tech Ltd.

Table 4 The relevant parameters of IJM device. The data was provided by Lumiere Tech Ltd.

Content	Parameter
Number of IJM	Up to 8
Number of pumps	Up to 16
Number of flow meters	Up to 16
Process connection inlet**	Sanitary Clamp Connector (2 inlets)
Process connection outlet**	Sanitary Clamp Connector (1 outlet)
Volumetric flow rate	Depending on configuration
Maximum operating pressure***	50–70 bar (725–1015 psi)
Liquid temperature range	4–60 °C (39.2–140 °F)
Wetted materials	Stainless steel, PEEK, titanium, FFKM, PTFE (GFP 55), aluminum oxide, ruby, sapphire, EPDM, zirconium oxide, POM, hastelloy
Power supply	Pump: 100–240 VAC single phase, 50/60 Hz; Flow meter: 115/230 VAC single phase; depending on configuration
Power consumption (per device)	Pump: maximum 320 W; flow meter: 3 W; PC: 1000 W; monitor: 380 W; network switch: 50 W
Ambient conditions	Temperature range: 4–40 °C; 39.2–104 °F; below 90% humidity (non-condensing)

IJM, impingement jet mixer; **, different connections on request; ***, depends on specific pump configuration and application.

Ltd. self-developed domestic high-throughput microfluidic device (INano™) to large-scale produce mRNA vaccines with lipopolyplex (LPP) as drug carrier²¹⁰. LPP nano-delivery platform is a double-layer structure with polymer-encapsulated mRNA as the core and phospholipid as the outer shell. Compared with traditional LNPs, LPP has better encapsulation and protection of mRNA, and can gradually release mRNA molecules when the polymer degrades. On April 29, 2022, StemiRNA Therapeutics Co., Ltd. announced that their self-developed mRNA vaccine against COVID-19 had been approved by State Food and Drug Administration (China) and would carry out clinical experiments²¹¹. Recently, Akso Biotechnology completed an angel round of financing of RMB 20 million to develop high-throughput 3D microfluidic chips, and accelerate the large-scale production of high-performance microspheres²¹².

Microfluidics-mediated NDDSs provide a firm foundation for the successful development and commercialization of COVID-19 vaccines, which is a key component in the rapid industrialization of COVID-19 vaccines. The unique large-scale production of microfluidics-mediated NDDSs is different from the scale-up process of traditional technology, which prominently shortens the translational time from laboratory preparation to industrial manufacturing, effectively accelerating the drug development and production progress. Recently, parallelization or numbering-up of microfluidic devices can scale up to produce microfluidics-mediated NDDSs. However, controllability still needs to be further attention. Therefore, combining the multidisciplinary advantages of nanotechnology, automation technology, and biomedicine, to develop intelligent and controllable microfluidics-mediated NDDSs will be helpful for further improvement of the production efficiency and homogeneity of the as-prepared drug delivery systems.

Although microfluidic-mediated LNPs have been used for the preparation of COVID-19 vaccines and the drug that suffered from polyneuropathy triggered by hATTR in industrial production, there are still some severe challenges that remain to be conquered. For instance, during the production process, Pfizer-BioNTech vaccine uses an IJM constructed from multiple static mixers in parallel for continuous production to improve the production efficiency of COVID-19 vaccine, but it still suffers from the possible failure of any one of the static mixers which may affect the quality and the production efficiency mRNA vaccines, which undoubtedly

increases the uncontrollability of production. Moreover, excessive production pressure greatly increases the risks met in the production process, and thus higher requirements for the stability of the equipment are required. Furthermore, at present, the purification process of the microfluidic-mediated NDDSs needs to be carried out separately after the synthesis process, which retards the production efficiency and increases the difficulty of preparation. Thus, in view of the above-mentioned problems during the industrial production process, the following points need to be further considered: 1) Multifunctional mixers with efficient, stable and smart production capabilities need to be researched and developed to improve the yields faced in large-scale industrial production. 2) The mixers for the production of microfluidic-mediated NDDSs need to be optimized through industrial design strategies, and more convenient and stable reactors need to be produced with the assistance of various technology, thereby effectively improving the safety in the industrial large-scale production process. 3) Reactors that can combine the synthesis and purification of microfluidic-mediated NDDSs to simplify the preparation process and improve production efficiency should be developed to serve as a reliable cornerstone for the industrial microfluidic-mediated NDDSs.

5. Conclusions and perspective

In this review, we have presented a comprehensive summary of microfluidics-based NDDSs, from fundamentals to industrialized applications. Because of its capabilities of miniaturization and precise control over fluids, microfluidics has an extremely important contribution to NDDSs. First, we reviewed the fundamentals of microfluidics. The fluid characteristic is laminar, and mass transfer is dominated by passive molecular diffusion. Microfluidics is divided into continuous-flow microfluidics and segmented-flow microfluidics. Continuous-flow microfluidics mainly focuses on miscible fluid. Owing to the simplicity of the flow pattern, the scaling-up of microfluidics-mediated NDDSs can be realized through increasing flow rate. The segmented-flow microfluidics mainly focuses on immiscible fluid, and it is able to produce monodisperse droplets with narrow size distribution. By continuously controlling the reaction condition, process parameters (*e.g.*, FRR, microfluidic device geometry, flow rate), and the mixing sequence of reagents during the reaction process,

microfluidics-mediated NDDSs with narrow particle size distribution, high drug-loading capacity can be controllably prepared. Therefore, microfluidics offers a new strategy for preparing NDDSs. Afterward, we summarize the microfluidic synthesis of NDDSs, including liposomes and nanoparticles (such as LNPs, PNPs, protein nanoparticles, and inorganic nanoparticles), and provide insights into the synthesis methods, existing problems, and research progress. Finally, the industrialization of microfluidics-mediated NDDSs is introduced. The success of Pfizer/BioNTech's BNT162b2 and Moderna's mRNA-1273 against COVID-19 demonstrated the feasibility of microfluidics for scaling up the preparation of NDDSs. Meanwhile, in China, some companies (e.g., StemiRNA Therapeutics Co., Ltd., micro&nano Biologics Co., Ltd., Akso Biotechnology, etc.) also apply microfluidic technology to produce microfluidic-based NDDSs, thereby accelerating the industrial development of microfluidics-mediated NDDSs.

Although microfluidics-mediated NDDSs have been used in industrial production, there are still some challenges to be overcome. Firstly, the hydrodynamic theory and growth mechanism of microfluidics-mediated NDDSs still need to be further explored to guide and optimize the carrier stability and drug loading issues during the construction of drug carriers. For example, rapid phase separation may easily lead to compact structures of the as-prepared nano drug carriers during the synthesis of microfluidics-mediated NDDSs. The flow behavior of liquids and the phase state changes of nanocarriers in numerous microfluidic devices can be further studied to establish a theoretical relationship between microfluidic systems and nanocarriers, thereby summarizing the design principles of the microfluidics-mediated NDDSs. Secondly, the fabrication process still needs to be further optimized. The physicochemical properties of NDDSs (e.g., size, morphology, dispersity) have a great impact on tissue distribution, blood circulating time and cellular internalization, etc. However, controllable preparation principles of microfluidics-mediated NDDSs are still not ideal. Therefore, more precise control over the physicochemical properties of microfluidics-mediated NDDSs still needs further exploration. In addition, organic solvents used as liquid phases may present poor biocompatibility and affect the biological activity of drugs, so liquid phases for fabricating microfluidics-mediated NDDSs with better biocompatibility still need to be further developed. Thirdly, microfluidic devices still need to be further designed. The material for microfluidic device fabrication is significantly important since the wetting and contact angles of solution may also affect the properties of microfluidics-mediated NDDSs. In order to meet the temperature and pressure conditions needed for fabricating NDDSs, other essential factors such as chemical compatibility, durability, and transparency must be also considered. The microfluidic devices with chaotic mixers are widely used to improve mixing efficiency between reagents. However, clogging problems often occur, thus limiting the production efficiency. Therefore, the geometry of microfluidic devices should also be further optimized. Last but not least, although the success of BNT162b2 and mRNA-1273 against COVID-19 demonstrates the feasibility of microfluidics for scaling up the preparation of NDDSs via parallelization or numbering-up, several challenges should still be considered. 1) Some laboratory-designed microfluidic devices ignore the practicality of industrial production. For instance, in order to solve clogging problems and increase the production efficiency of microfluidics-mediated NDDSs, a 3D-HFF microfluidic device has been used in the laboratory. However, how the microfluidic device can be parallelized or numbered up in industrial

production to achieve scale-up should be further considered. 2) Most of the current microfluidics-mediated NDDSs need further off-chip purification. Moreover, integrated multi-process microfluidic systems can be designed, and this will shorten processing time and improve production efficiency. 3) Microfluidic devices rely on customized modular components, and chips for liquid mixing suffer from vulnerable materials, complex design, and small liquid flow, which greatly limit the large-scale industrial production of microfluidics-mediated NDDSs. Therefore, combining the advantages of materials science, synthetic science, and industrial production to design microfluidic chips equipped with high-pressure resistance, corrosion resistance, and continuous generation, will serve as a reliable cornerstone for the industrial microfluidics-mediated NDDSs. Overall, although microfluidics still exists some challenges, it provides an excellent strategy to controllably prepare NDDSs.

Acknowledgments

This review paper was supported by the projects of National Natural Science Foundation of China (No. 82073784, China), Jilin Province Science and Technology Development Program (No. 20200801012GH, China) and Industrial Technology Research and Development Projects from the Development and Reform Commission of Jilin Province Major Science and Technology Special Projects (20200504005YY, China). Fig. 1 was created with BioRender.com.

Author contributions

In this article, each author participated in article preparation. Huan Zhang and Lesheng Teng designed the review. Huan Zhang wrote part of the introduction and the fundamentals of microfluidics. Rongze Sun and Songren Han wrote part of the microfluidic synthesis of NDDSs. Jie Yang wrote part of the industrialization and challenges of microfluidic-mediated NDDSs. Zhaogang Yang reviewed this manuscript. Huan Zhang, Zhaogang Yang and Lesheng Teng revised the manuscript. All of the authors have read and approved the final manuscript.

Conflicts of interest

The authors have no conflicts of interest to declare.

References

1. Amirifar L, Besanjideh M, Nasiri R, Shamloo A, Nasrollahi F, de Barros NR, et al. Droplet-based microfluidics in biomedical applications. *Biofabrication* 2022;**14**:022001.
2. Ma Q, Cao J, Gao Y, Han S, Liang Y, Zhang T, et al. Microfluidic-mediated nano-drug delivery systems: from fundamentals to fabrication for advanced therapeutic applications. *Nanoscale* 2020;**12**:15512–27.
3. Mahhengam N, Fahem Ghetran Khazaali A, Aravindhan S, Olegovna Zekiy A, Melnikova L, Siahmansouri H. Applications of microfluidic devices in the diagnosis and treatment of cancer: a review study. *Crit Rev Anal Chem* 2022;**52**:1863–77.
4. Liu Y, Sun L, Zhang H, Shang L, Zhao Y. Microfluidics for drug development: from synthesis to evaluation. *Chem Rev* 2021;**121**:7468–529.
5. Chen Z, Lan Y, Ling SD, Dong YH, Wang YD, Xu JH. Microfluidic-generated biopolymer microparticles as cargo delivery systems. *Adv Mater Technol* 2022;**7**:2100733.

6. Sanjay ST, Zhou W, Dou M, Tavakoli H, Ma L, Xu F, et al. Recent advances of controlled drug delivery using microfluidic platforms. *Adv Drug Deliv Rev* 2018;**128**:3–28.
7. Martins JP, Torrieri G, Santos HA. The importance of microfluidics for the preparation of nanoparticles as advanced drug delivery systems. *Expert Opin Drug Deliv* 2018;**15**:469–79.
8. Manz A, Graber N, Widmer HÁ. Miniaturized total chemical analysis systems: a novel concept for chemical sensing. *Sens Actuators, B* 1990;**1**:244–8.
9. Manz A, Miyahara Y, Miura J, Watanabe Y, Miyagi H, Sato K. Design of an open-tubular column liquid chromatograph using silicon chip technology. *Sens Actuators, B* 1990;**1**:249–55.
10. Miniaturization of chemical analysis systems—a look into next century's technology or just a fashionable craze?. *Chimia* 1991;**45**:103.
11. Sharma B, Sharma A. Microfluidics: recent advances toward lab-on-chip applications in bioanalysis. *Adv Eng Mater* 2022;**24**:2100738.
12. Whitesides GM. The origins and the future of microfluidics. *Nature* 2006;**442**:368–73.
13. Xing G, Zhang W, Li N, Pu Q, Lin J-M. Recent progress on microfluidic biosensors for rapid detection of pathogenic bacteria. *Chin Chem Lett* 2022;**33**:1743–51.
14. Tsui JH, Lee W, Pun SH, Kim J, Kim DH. Microfluidics-assisted *in vitro* drug screening and carrier production. *Adv Drug Deliv Rev* 2013;**65**:1575–88.
15. Kang S, Park SE, Huh DD. Organ-on-a-chip technology for nanoparticle research. *Nano Converg* 2021;**8**:20.
16. Karam M, Daoud G. mRNA vaccines: past, present, future. *Asian J Pharm Sci* 2022;**17**:491–522.
17. Tokeshi M. Microfluidic devices for drug delivery systems. *Adv Drug Deliv Rev* 2018;**128**:1–2.
18. Tseng YC, Mozumdar S, Huang L. Lipid-based systemic delivery of siRNA. *Adv Drug Deliv Rev* 2009;**61**:721–31.
19. Yuan XL, Zhu Y, Li SS, Wu YQ, Wang ZS, Gao R, et al. Titanium nanosheet as robust and biosafe drug carrier for combined photochemo cancer therapy. *J Nanobiotechnol* 2022;**20**:154.
20. Yi SH, Liao RQ, Zhao W, Huang YS, He Y. Multifunctional co-transport carriers based on cyclodextrin assembly for cancer synergistic therapy. *Theranostics* 2022;**12**:2560–79.
21. Magar KT, Boafu GF, Li XT, Chen ZJ, He W. Liposome-based delivery of biological drugs. *Chin Chem Lett* 2022;**33**:587–96.
22. Khan NH, Mir M, Qian L, Baloch M, Khan MFA, Rehman AU, et al. Skin cancer biology and barriers to treatment: recent applications of polymeric micro/nanostructures. *J Adv Res* 2021;**36**:223–47.
23. Wang L, Li YZ, Ren MX, Wang X, Li LJ, Liu FY, et al. pH and lipase-responsive nanocarrier-mediated dual drug delivery system to treat periodontitis in diabetic rats. *Bioact Mater* 2022;**18**:254–66.
24. Cao MZ, Zhan ML, Wang Z, Wang ZQ, Li XM, Miao MS. Development of an orally bioavailable isoliquiritigenin self-nanoemulsifying drug delivery system to effectively treat ovalbumin-induced asthma. *Int J Nanomed* 2020;**15**:8945–61.
25. Asfour MH, Kassem AA, Salama A, Abd El-Alim SH. Hydrophobic ion pair loaded self-emulsifying drug delivery system (SEDDS): a novel oral drug delivery approach of cromolyn sodium for management of bronchial asthma. *Int J Pharm* 2020;**585**:119494.
26. Choi A, Seo KD, Kim DW, Kim BC, Kim DS. Recent advances in engineering microparticles and their nascent utilization in biomedical delivery and diagnostic applications. *Lab Chip* 2017;**17**:591–613.
27. Berkland C, King M, Cox A, Kim K, Pack DW. Precise control of PLG microsphere size provides enhanced control of drug release rate. *J Control Release* 2002;**82**:137–47.
28. Liu D, Zhang H, Fontana F, Hirvonen JT, Santos HA. Microfluidic-assisted fabrication of carriers for controlled drug delivery. *Lab Chip* 2017;**17**:1856–83.
29. Zhang L, Chen Q, Ma Y, Sun J. Microfluidic methods for fabrication and engineering of nanoparticle drug delivery systems. *ACS Appl Bio Mater* 2020;**3**:107–20.
30. Capretto L, Carugo D, Mazzitelli S, Nastruzzi C, Zhang X. Microfluidic and lab-on-a-chip preparation routes for organic nanoparticles and vesicular systems for nanomedicine applications. *Adv Drug Deliv Rev* 2013;**65**:1496–532.
31. Shrimal P, Jadeja G, Patel S. A review on novel methodologies for drug nanoparticle preparation: microfluidic approach. *Chem Eng Res Des* 2020;**153**:728–56.
32. Zhang H, Zhu Y, Shen Y. Microfluidics for cancer nanomedicine: from fabrication to evaluation. *Small* 2018;**14**:e1800360.
33. Bernal JL, Andrews N, Gower C, Gallagher E, Simmons R, Thelwall S, et al. Effectiveness of Covid-19 vaccines against the B.1.617.2 (Delta) variant. *N Engl J Med* 2021;**385**:585–94.
34. Stroock AD, Dertinger SK, Ajdari A, Mezic I, Stone HA, Whitesides GM. Chaotic mixer for microchannels. *Science* 2002;**295**:647–51.
35. Sharp KV, Adrian RJ. Transition from laminar to turbulent flow in liquid filled microtubes. *Exp Fluid* 2004;**36**:741–7.
36. Liu D, Zhang H, Fontana F, Hirvonen JT, Santos HA. Current developments and applications of microfluidic technology toward clinical translation of nanomedicines. *Adv Drug Deliv Rev* 2018;**128**:54–83.
37. Fabozzi A, Della Sala F, di Gennaro M, Solimando N, Pagliuca M, Borzacchiello A. Polymer based nanoparticles for biomedical applications by microfluidic techniques: from design to biological evaluation. *Polym Chem* 2021;**12**:6667–87.
38. Atencia J, Beebe DJ. Controlled microfluidic interfaces. *Nature* 2005;**437**:648–55.
39. Glass KKF, Longmire EK, Hubel A. Optimization of a microfluidic device for diffusion-based extraction of DMSO from a cell suspension. *Int J Heat Mass Tran* 2008;**51**:5749–57.
40. Suzuki H, Ho CM, Kasagi N. A chaotic mixer for magnetic bead-based micro cell sorter. *J Microelectromech Syst* 2004;**13**:779–90.
41. Damiati S, Kompella UB, Damiati SA, Kodzius R. Microfluidic devices for drug delivery systems and drug screening. *Genes* 2018;**9**:103.
42. Kimura N, Maeki M, Sato Y, Note Y, Ishida A, Tani H, et al. Development of the iLiNP device: fine tuning the lipid nanoparticle size within 10 nm for drug delivery. *ACS Omega* 2018;**3**:5044–51.
43. Hood RR, DeVoe DL, Atencia J, Vreeland WN, Omiatek DM. A facile route to the synthesis of monodisperse nanoscale liposomes using 3D microfluidic hydrodynamic focusing in a concentric capillary array. *Lab Chip* 2014;**14**:2403–9.
44. Jahn A, Vreeland WN, Gaitan M, Locascio LE. Controlled vesicle self-assembly in microfluidic channels with hydrodynamic focusing. *J Am Chem Soc* 2004;**126**:2674–5.
45. Mitchell MJ, Jain RK, Langer R. Engineering and physical sciences in oncology: challenges and opportunities. *Nat Rev Cancer* 2017;**17**:659–75.
46. Rhee M, Valencia PM, Rodriguez MI, Langer R, Farokhzad OC, Karnik R. Synthesis of size-tunable polymeric nanoparticles enabled by 3D hydrodynamic flow focusing in single-layer microchannels. *Adv Mater* 2011;**23**:H79–83.
47. Ahn J, Ko J, Lee S, Yu J, Kim Y, Jeon NL. Microfluidics in nanoparticle drug delivery; from synthesis to pre-clinical screening. *Adv Drug Deliv Rev* 2018;**128**:29–53.
48. Li Y, Lee RJ, Huang X, Li Y, Lv B, Wang T, et al. Single-step microfluidic synthesis of transferrin-conjugated lipid nanoparticles for siRNA delivery. *Nanomedicine* 2017;**13**:371–81.
49. Sun YT, Lee RJ, Meng FC, Wang GY, Zheng XL, Dong SY, et al. Microfluidic self-assembly of high cabazitaxel loading albumin nanoparticles. *Nanoscale* 2020;**12**:16928–33.
50. Maeki M, Kimura N, Sato Y, Harashima H, Tokeshi M. Advances in microfluidics for lipid nanoparticles and extracellular vesicles and applications in drug delivery systems. *Adv Drug Deliv Rev* 2018;**128**:84–100.
51. Maeki M, Saito T, Sato Y, Yasui T, Kaji N, Ishida A, et al. A strategy for synthesis of lipid nanoparticles using microfluidic devices with a mixer structure. *RSC Adv* 2015;**5**:46181–5.
52. Maeki M, Fujishima Y, Sato Y, Yasui T, Kaji N, Ishida A, et al. Understanding the formation mechanism of lipid nanoparticles in

- microfluidic devices with chaotic micromixers. *PLoS One* 2017;**12**: e0187962.
53. Tao J, Chow SF, Zheng Y. Application of flash nanoprecipitation to fabricate poorly water-soluble drug nanoparticles. *Acta Pharm Sin B* 2019;**9**:4–18.
 54. Teh SY, Lin R, Hung LH, Lee AP. Droplet microfluidics. *Lab Chip* 2008;**8**:198–220.
 55. Zhao CX. Multiphase flow microfluidics for the production of single or multiple emulsions for drug delivery. *Adv Drug Deliv Rev* 2013; **65**:1420–46.
 56. Nunes JK, Tsai SSH, Wan J, Stone HA. Dripping and jetting in microfluidic multiphase flows applied to particle and fiber synthesis. *J Phys D Appl Phys* 2013;**46**:114002.
 57. Wang W, Zhang M-J, Chu LY. Functional polymeric microparticles engineered from controllable microfluidic emulsions. *Acc Chem Res* 2014;**47**:373–84.
 58. Czekalska MA, Jacobs AMJ, Toprakcioglu Z, Kong L, Baumann KN, Gang H, et al. One-step generation of multisomes from lipid-stabilized double emulsions. *ACS Appl Mater Interfaces* 2021;**13**:6739–47.
 59. Ran R, Middelberg API, Zhao CX. Microfluidic synthesis of multi-functional liposomes for tumour targeting. *Colloids Surf B Biointerfaces* 2016;**148**:402–10.
 60. Lee CY, Tsai T, Peng PC, Chen CT. Fabrication of doxorubicin-loaded lipid-based nanocarriers by microfluidic rapid mixing. *Biomedicines* 2022;**10**:1259.
 61. Hamano N, Bottger R, Lee SE, Yang Y, Kulkarni JA, Ip S, et al. Robust microfluidic technology and new lipid composition for fabrication of curcumin-loaded liposomes: effect on the anticancer activity and safety of cisplatin. *Mol Pharm* 2019;**16**:3957–67.
 62. Lv S, Jing R, Liu X, Shi H, Shi Y, Wang X, et al. One-step microfluidic fabrication of multi-responsive liposomes for targeted delivery of doxorubicin synergism with photothermal effect. *Int J Nanomed* 2021;**16**:7759–72.
 63. Michelon M, Oliveira DRB, de Figueiredo Furtado G, Gaziola de la Torre L, Cunha RL. High-throughput continuous production of liposomes using hydrodynamic flow-focusing microfluidic devices. *Colloids Surf B Biointerfaces* 2017;**156**:349–57.
 64. Lin WS, Malmstadt N. Liposome production and concurrent loading of drug simulants by microfluidic hydrodynamic focusing. *Eur Biophys J* 2019;**48**:549–58.
 65. Sedighi M, Sieber S, Rahimi F, Shahbazi MA, Rezayan AH, Huwlyer J, et al. Rapid optimization of liposome characteristics using a combined microfluidics and design-of-experiment approach. *Drug Deliv Transl Res* 2019;**9**:404–13.
 66. Belliveau NM, Huft J, Lin PJC, Chen S, Leung AKK, Leaver TJ, et al. Microfluidic synthesis of highly potent limit-size lipid nanoparticles for *in vivo* delivery of siRNA. *Mol Ther Nucleic Acids* 2012; **1**:e37.
 67. Roces CB, Lou G, Jain N, Abraham S, Thomas A, Halbert GW, et al. Manufacturing considerations for the development of lipid nanoparticles using microfluidics. *Pharmaceutics* 2020;**12**:1095.
 68. Shepherd SJ, Warzecha CC, Yadavali S, El-Mayta R, Alameh M-G, Wang L, et al. Scalable mRNA and siRNA lipid nanoparticle production using a parallelized microfluidic device. *Nano Lett* 2021;**21**: 5671–80.
 69. Arduino I, Liu Z, Rahikkala A, Figueiredo P, Correia A, Cutrignelli A, et al. Preparation of cetyl palmitate-based PEGylated solid lipid nanoparticles by microfluidic technique. *Acta Biomater* 2021;**121**:566–78.
 70. Okuda K, Sato Y, Iwakawa K, Sasaki K, Okabe N, Maeki M, et al. On the size-regulation of RNA-loaded lipid nanoparticles synthesized by microfluidic device. *J Control Release* 2022;**348**:648–59.
 71. Meng FC, Sun YT, Lee RJ, Wang GY, Zheng XL, Zhang H, et al. Folate Receptor-targeted albumin nanoparticles based on microfluidic technology to deliver cabazitaxel. *Cancers* 2019;**11**:1571.
 72. Pourabed A, Younas T, Liu C, Shanbhag BK, He L, Alan T. High throughput acoustic microfluidic mixer controls self-assembly of protein nanoparticles with tuneable sizes. *J Colloid Interface Sci* 2021;**585**:229–36.
 73. Zhang L, Beatty A, Lu L, Abdalrahman A, Makris TM, Wang G, et al. Microfluidic-assisted polymer-protein assembly to fabricate homogeneous functional nanoparticles. *Mater Sci Eng C Mater Biol Appl* 2020;**111**:110768.
 74. Zhang H, Wang T, He F, Chen G. Fabrication of pea protein-curcumin nanocomplexes via microfluidization for improved solubility, nano-dispersibility and heat stability of curcumin: insight on interaction mechanisms. *Int J Biol Macromol* 2021;**168**:686–94.
 75. Hu G, Yang L, Li Y, Wang L. Continuous and scalable fabrication of stable and biocompatible MOF@SiO₂ nanoparticles for drug loading. *J Mater Chem B* 2018;**6**:7936–42.
 76. Xu XY, Koivisto O, Liu C, Zhou JN, Miihkinen M, Jacquemet G, et al. Effective delivery of the CRISPR/CAS9 system enabled by functionalized mesoporous silica nanoparticles for GFP-tagged paxillin knock-in. *Adv Ther* 2021;**4**:2000072.
 77. Gaikwad G, Bangde P, Rane K, Stenberg J, Borde L, Bhagwat S, et al. Continuous production and separation of new biocompatible palladium nanoparticles using a droplet microreactor. *Microfluid Nanofluidics* 2021;**25**:27.
 78. Liu Z, Li Y, Li W, Xiao C, Liu D, Dong C, et al. Multifunctional nanohybrid based on porous silicon nanoparticles, gold nanoparticles, and acetalated dextran for liver regeneration and acute liver failure theranostics. *Adv Mater* 2018;**30**:e1703393.
 79. Bresseleers J, Bagheri M, Lebleu C, Lecommandoux S, Sandre O, Pijpers IAB, et al. Tuning size and morphology of mPEG-*b*-p(HPMA-Bz) copolymer self-assemblies using microfluidics. *Polymers* 2020;**12**:2572.
 80. Wang Y, Thies-Weesie DME, Bosman EDC, van Steenberg MJE, van den Dikkenberg J, Shi Y, et al. Tuning the size of all-HPMA polymeric micelles fabricated by solvent extraction. *J Control Release* 2022;**343**:338–46.
 81. Bao Y, Deng Q, Li Y, Zhou S. Engineering docetaxel-loaded micelles for non-small cell lung cancer: a comparative study of microfluidic and bulk nanoparticle preparation. *RSC Adv* 2018;**8**:31950–66.
 82. Maravajjala KS, Swetha KL, Sharma S, Padhye T, Roy A. Development of a size-tunable paclitaxel micelle using a microfluidic-based system and evaluation of its *in-vitro* efficacy and intracellular delivery. *J Drug Deliv Sci Technol* 2020;**60**: 102041.
 83. Abad M, Mendoza G, Uson L, Arruebo M, Pinol M, Sebastian V, et al. Microfluidic synthesis of block copolymer micelles: application as drug nanocarriers and as photothermal transducers when loading Pd nanosheets. *Macromol Biosci* 2022;**22**:e2100528.
 84. Baby T, Liu Y, Yang G, Chen D, Zhao CX. Microfluidic synthesis of curcumin loaded polymer nanoparticles with tunable drug loading and pH-triggered release. *J Colloid Interface Sci* 2021;**594**:474–84.
 85. Huang Y, Jazani AM, Howell EP, Oh JK, Moffitt MG. Controlled microfluidic synthesis of biological stimuli-responsive polymer nanoparticles. *ACS Appl Mater Interfaces* 2020;**12**:177–90.
 86. Cao Y, Silverman L, Lu C, Hof R, Wulff JE, Moffitt MG. Microfluidic manufacturing of SN-38-loaded polymer nanoparticles with shear processing control of drug delivery properties. *Mol Pharm* 2019;**16**:96–107.
 87. Ferezou J, Bach AC. Structure and metabolic fate of triacylglycerol- and phospholipid-rich particles of commercial parenteral fat emulsions. *Nutrition* 1999;**15**:44–50.
 88. Wang DY, van der Mei HC, Ren Y, Busscher HJ, Shi L. Lipid-based antimicrobial delivery-systems for the treatment of bacterial infections. *Front Chem* 2019;**7**:872.
 89. Li S, Yin G, Pu X, Huang Z, Liao X, Chen X. A novel tumor-targeted thermosensitive liposomal cerasome used for thermally controlled drug release. *Int J Pharm* 2019;**570**:118660.
 90. Daeihamed M, Dadashzadeh S, Haeri A, Akhlaghi MF. Potential of liposomes for enhancement of oral drug absorption. *Curr Drug Deliv* 2017;**14**:289–303.

91. Park W, Na K. Advances in the synthesis and application of nanoparticles for drug delivery. *Wiley Interdiscip Rev Nanomed Nanobiotechnol* 2015;**7**:494–508.
92. Plaza-Oliver M, Santander-Ortega MJ, Lozano MV. Current approaches in lipid-based nanocarriers for oral drug delivery. *Drug Deliv Transl Res* 2021;**11**:471–97.
93. Kusunose J, Zhang H, Gagnon MK, Pan T, Simon SI, Ferrara KW. Microfluidic system for facilitated quantification of nanoparticle accumulation to cells under laminar flow. *Ann Biomed Eng* 2013;**41**:89–99.
94. Obeid MA, Teeravatcharoenchai T, Connell D, Niwasabutra K, Hussain M, Carter K, et al. Examination of the effect of niosome preparation methods in encapsulating model antigens on the vesicle characteristics and their ability to induce immune responses. *J Liposome Res* 2021;**31**:195–202.
95. Ilhan-Ayisigi E, Ghazal A, Sartori B, Dimaki M, Svendsen WE, Yesil-Celiktas O, et al. Continuous microfluidic production of citremphosphatidylcholine nano-self-assemblies for thymoquinone delivery. *Nanomaterials* 2021;**11**:1510.
96. Jahn A, Stavits SM, Hong JS, Vreeland WN, DeVoe DL, Gaitan M. Microfluidic mixing and the formation of nanoscale lipid vesicles. *ACS Nano* 2010;**4**:2077–87.
97. Zizzari A, Bianco M, Carbone L, Perrone E, Amato F, Maruccio G, et al. Continuous-flow production of injectable liposomes via a microfluidic approach. *Materials* 2017;**10**:1411.
98. Chen Z, Han JY, Shumate L, Fedak R, DeVoe DL. High throughput nanoliposome formation using 3D printed microfluidic flow focusing chips. *Adv Mater Technol* 2019;**4**:1800511.
99. Balbino TA, Serafin JM, Radaic A, de Jesus MB, de la Torre LG. Integrated microfluidic devices for the synthesis of nanoscale liposomes and lipoplexes. *Colloids Surf B Biointerfaces* 2017;**152**:406–13.
100. Kastner E, Verma V, Lowry D, Perrie Y. Microfluidic-controlled manufacture of liposomes for the solubilisation of a poorly water soluble drug. *Int J Pharm* 2015;**485**:122–30.
101. Zhang L, Feng Q, Wang J, Sun J, Shi X, Jiang X. Microfluidic synthesis of rigid nanovesicles for hydrophilic reagents delivery. *Angew Chem Int Ed Engl* 2015;**54**:3952–6.
102. Bottom-up assembly of functional intracellular synthetic organelles by droplet-based microfluidics. *Small* 2020;**16**:e1906424.
103. Deshpande S, Dekker C. On-chip microfluidic production of cell-sized liposomes. *Nat Protoc* 2018;**13**:856–74.
104. Van de Cauter L, Fanalista F, van Buren L, De Franceschi N, Godino E, Bouw S, et al. Optimized cDICE for efficient reconstitution of biological systems in giant unilamellar vesicles. *ACS Synth Biol* 2021;**10**:1690–702.
105. Dimitriou P, Li J, Tornillo G, McCloy T, Barrow D. Droplet microfluidics for tumor drug-related studies and programmable artificial cells. *Glob Chall* 2021;**5**:2000123.
106. Boraschi D, Italiani P, Palomba R, Decuzzi P, Duschl A, Fadeel B, et al. Nanoparticles and innate immunity: new perspectives on host defence. *Semin Immunol* 2017;**34**:33–51.
107. Ftouh M, Kalboussi N, Abid N, Sfar S, Mignet N, Bahloul B. Contribution of nanotechnologies to vaccine development and drug delivery against respiratory viruses. *PPAR Res* 2021;**2021**:6741290.
108. Samaridou E, Heyes J, Lutwyche P. Lipid nanoparticles for nucleic acid delivery: current perspectives. *Adv Drug Deliv Rev* 2020;**154–155**:37–63.
109. Shankar R, Joshi M, Pathak K. Lipid nanoparticles: a novel approach for brain targeting. *Pharm Nanotechnol* 2018;**6**:81–93.
110. Fan Y, Marioli M, Zhang K. Analytical characterization of liposomes and other lipid nanoparticles for drug delivery. *J Pharm Biomed Anal* 2021;**192**:113642.
111. Wang WH, Huang ZW, Li YB, Wang WH, Shi JY, Fu FQ, et al. Impact of particle size and pH on protein corona formation of solid lipid nanoparticles: a proof-of-concept study. *Acta Pharm Sin B* 2021;**11**:1030–46.
112. Solid lipid nanoparticles for dibucaine sustained release. *Pharmaceutics* 2018;**10**:231.
113. Kumar R, Singh A, Garg N. Acoustic cavitation-assisted formulation of solid lipid nanoparticles using different stabilizers. *ACS Omega* 2019;**4**:13360–70.
114. Pizzolo CD, Filippin-Monteiro FB, Restrepo JA, Pittella F, Silva AH, Alves de Souza P, et al. Influence of surfactant and lipid type on the physicochemical properties and biocompatibility of solid lipid nanoparticles. *Int J Environ Res Publ Health* 2014;**11**:8581–96.
115. Ball RL, Bajaj P, Whitehead KA. Achieving long-term stability of lipid nanoparticles: examining the effect of pH, temperature, and lyophilization. *Int J Nanomed* 2016;**12**:305–15.
116. Muramatsu H, Lam K, Bajusz C, Laczko D, Karikó K, Schreiner P, et al. Lyophilization provides long-term stability for a lipid nanoparticle-formulated, nucleoside-modified mRNA vaccine. *Mol Ther* 2022;**30**:1941–51.
117. Carvalho BG, Ceccato BT, Michelon M, Han SW, De la Torre LG. Advanced microfluidic technologies for lipid nano-microsystems from synthesis to biological application. *Pharmaceutics* 2022;**14**:141.
118. Mandal B, Bhattacharjee H, Mittal N, Sah H, Balabathula P, Thoma LA, et al. Core-shell-type lipid-polymer hybrid nanoparticles as a drug delivery platform. *Nanomedicine* 2013;**9**:474–91.
119. Mu H, Holm R. Solid lipid nanocarriers in drug delivery: characterization and design. *Expert Opin Drug Deliv* 2018;**15**:771–85.
120. Scioli Montoto S, Muraca G, Ruiz ME. Solid lipid nanoparticles for drug delivery: pharmacological and biopharmaceutical aspects. *Front Mol Biosci* 2020;**7**:587997.
121. Banerjee S, Pillai J. Solid lipid matrix mediated nanoarchitectonics for improved oral bioavailability of drugs. *Expert Opin Drug Metabol Toxicol* 2019;**15**:499–515.
122. Bost JP, Barriga H, Holme MN, Gallud A, Maugeri M, Gupta D, et al. Delivery of oligonucleotide therapeutics: chemical modifications, lipid nanoparticles, and extracellular vesicles. *ACS Nano* 2021;**15**:13993–4021.
123. Witzigmann D, Kulkarni JA, Leung J, Chen S, Cullis PR, van der Meel R. Lipid nanoparticle technology for therapeutic gene regulation in the liver. *Adv Drug Deliv Rev* 2020;**159**:344–63.
124. Alavi M, Hamidi M. Passive and active targeting in cancer therapy by liposomes and lipid nanoparticles. *Drug Metab Pers Ther* 2019;**34**:20180032.
125. Riewe J, Erfle P, Melzig S, Kwade A, Dietzel A, Bunjes H. Antisolvent precipitation of lipid nanoparticles in microfluidic systems - a comparative study. *Int J Pharm* 2020;**579**:119167.
126. Maugeri M, Nawaz M, Papadimitriou A, Angerfors A, Camponeschi A, Na M, et al. Linkage between endosomal escape of LNP-mRNA and loading into EVs for transport to other cells. *Nat Commun* 2019;**10**:4333.
127. Fan Y, Yen CW, Lin HC, Hou W, Estevez A, Sarode A, et al. Automated high-throughput preparation and characterization of oligonucleotide-loaded lipid nanoparticles. *Int J Pharm* 2021;**599**:120392.
128. Nakamura T, Kawai M, Sato Y, Maeki M, Tokeshi M, Harashima H. The effect of size and charge of lipid nanoparticles prepared by microfluidic mixing on their lymph node transitivity and distribution. *Mol Pharm* 2020;**17**:944–53.
129. Terada T, Kulkarni JA, Huynh A, Chen S, van der Meel R, Tam YYC, et al. Characterization of lipid nanoparticles containing ionizable cationic lipids using design-of-experiments approach. *Langmuir* 2021;**37**:1120–8.
130. Kimura N, Maeki M, Sato Y, Ishida A, Tani H, Harashima H, et al. Development of a microfluidic-based post-treatment process for size-controlled lipid nanoparticles and application to siRNA delivery. *ACS Appl Mater Interfaces* 2020;**12**:34011–20.
131. Ban J, Zhang Y, Huang X, Deng G, Hou D, Chen Y, et al. Corneal permeation properties of a charged lipid nanoparticle carrier containing dexamethasone. *Int J Nanomed* 2017;**12**:1329–39.
132. Cao H, Wang Y, Luan N, Liu C. Immunogenicity of varicella-zoster virus glycoprotein e formulated with lipid nanoparticles and nucleic immunostimulators in mice. *Vaccines* 2021;**9**:310.

133. Zhigaltsev IV, Tam YYC, Kulkarni JA, Cullis PR. Synthesis and characterization of hybrid lipid nanoparticles containing gold nanoparticles and a weak base drug. *Langmuir* 2022;**38**:7858–66.
134. Polymeric nanoparticles: production, characterization, toxicology and ecotoxicology. *Molecules* 2020;**25**:3731.
135. Musyanovych A, Landfester K. Polymer micro- and nanocapsules as biological carriers with multifunctional properties. *Macromol Biosci* 2014;**14**:458–77.
136. Xia W, Tao Z, Zhu B, Zhang W, Liu C, Chen S, et al. Targeted delivery of drugs and genes using polymer nanocarriers for cancer therapy. *Int J Mol Sci* 2021;**22**:9118.
137. Mainini F, Eccles MR. Lipid and polymer-based nanoparticle siRNA delivery systems for cancer therapy. *Molecules* 2020;**25**:2692.
138. Thomsen T, Ayoub AB, Psaltis D, Klok HA. Fluorescence-based and fluorescent label-free characterization of polymer nanoparticle decorated T cells. *Biomacromolecules* 2021;**22**:190–200.
139. Gagliardi M, Borri C. Polymer Nanoparticles as smart carriers for the enhanced release of therapeutic agents to the CNS. *Curr Pharmaceut Des* 2017;**23**:393–410.
140. Chowdhury P, Nagesh PKB, Khan S, Hafeez BB, Chauhan SC, Jaggi M, et al. Development of polyvinylpyrrolidone/paclitaxel self-assemblies for breast cancer. *Acta Pharm Sin B* 2018;**8**:602–14.
141. Yu M, Xue Y, Ma PX, Mao C, Lei B. Intrinsic ultrahigh drug/miRNA loading capacity of biodegradable bioactive glass nanoparticles toward highly efficient pharmaceutical delivery. *ACS Appl Mater Interfaces* 2017;**9**:8460–70.
142. Fernando LP, Kandel PK, Yu J, McNeill J, Ackroyd PC, Christensen KA. Mechanism of cellular uptake of highly fluorescent conjugated polymer nanoparticles. *Biomacromolecules* 2010;**11**:2675–82.
143. Rossi F, Ferrari R, Castiglione F, Mele A, Perale G, Moscatelli D. Polymer hydrogel functionalized with biodegradable nanoparticles as composite system for controlled drug delivery. *Nanotechnology* 2015;**26**:015602.
144. Ledet GA, Graves RA, Glotser EY, Mandal TK, Bostanian LA. Preparation and *in vitro* evaluation of hydrophilic fenretinide nanoparticles. *Int J Pharm* 2015;**479**:329–37.
145. Xue C, Shi X, Tian Y, Zheng X, Hu G. Diffusion of nanoparticles with activated hopping in crowded polymer solutions. *Nano Lett* 2020;**20**:3895–904.
146. Preparation of nanodispersions by solvent displacement using the Venturi tube. *Int J Pharm* 2018;**545**:254–60.
147. Date T, Nimbalkar V, Kamat J, Mittal A, Mahato RI, Chitkara D. Lipid-polymer hybrid nanocarriers for delivering cancer therapeutics. *J Control Release* 2018;**271**:60–73.
148. Huang Y, Jazani AM, Howell EP, Reynolds LA, Oh JK, Moffitt MG. Microfluidic shear processing control of biological reduction stimulus-responsive polymer nanoparticles for drug delivery. *ACS Biomater Sci Eng* 2020;**6**:5069–83.
149. Tahir N, Madni A, Li W, Correia A, Khan MM, Rahim MA, et al. Microfluidic fabrication and characterization of Sorafenib-loaded lipid-polymer hybrid nanoparticles for controlled drug delivery. *Int J Pharm* 2020;**581**:119275.
150. Ding Y, Wan J, Zhang Z, Wang F, Guo J, Wang C. Localized Fe(II)-induced cytotoxic reactive oxygen species generating nanosystem for enhanced anticancer therapy. *ACS Appl Mater Interfaces* 2018;**10**:4439–49.
151. Biocompatible gemcitabine-based nanomedicine engineered by flow focusing for efficient antitumor activity. *Int J Pharm* 2013;**443**:103–9.
152. Prabha S, Arya G, Chandra R, Ahmed B, Nimesh S. Effect of size on biological properties of nanoparticles employed in gene delivery. *Artif Cell Nanomed Biotechnol* 2016;**44**:83–91.
153. Gimondi S, Guimaraes CF, Vieira SF, Goncalves VMF, Tiritan ME, Reis RL, et al. Microfluidic mixing system for precise PLGA-PEG nanoparticles size control. *Nanomedicine* 2022;**40**:102482.
154. Iwasaki Y, Sawada S, Ishihara K, Khang G, Lee HB. Reduction of surface-induced inflammatory reaction on PLGA/MPC polymer blend. *Biomaterials* 2002;**23**:3897–903.
155. Martins C, Sarmento B. Microfluidic manufacturing of multitargeted PLGA/PEG nanoparticles for delivery of taxane chemotherapeutics. *Methods Mol Biol* 2020;**2059**:213–24.
156. Karnik R, Gu F, Basto P, Cannizzaro C, Dean L, Kyei-Manu W, et al. Microfluidic platform for controlled synthesis of polymeric nanoparticles. *Nano Lett* 2008;**8**:2906–12.
157. Leung MHM, Shen AQ. Microfluidic assisted nanoprecipitation of PLGA nanoparticles for curcumin delivery to leukemia jurkat cells. *Langmuir* 2018;**34**:3961–70.
158. Zoqlam R, Morris CJ, Akbar M, Alkilany AM, Hamdallah SI, Belton P, et al. Evaluation of the benefits of microfluidic-assisted preparation of polymeric nanoparticles for DNA delivery. *Mater Sci Eng C Mater Biol Appl* 2021;**127**:112243.
159. Li X, Jiang X. Microfluidics for producing poly (lactic-co-glycolic acid)-based pharmaceutical nanoparticles. *Adv Drug Deliv Rev* 2018;**128**:101–14.
160. Liu D, Cito S, Zhang Y, Wang C-F, Sikanen TM, Santos HA. A versatile and robust microfluidic platform toward high throughput synthesis of homogeneous nanoparticles with tunable properties. *Adv Mater* 2015;**27**:2298–304.
161. Yewale C, Baradia D, Vhora I, Misra A. Proteins: emerging carrier for delivery of cancer therapeutics. *Expert Opin Drug Deliv* 2013;**10**:1429–48.
162. Ge J, Neofytou E, Lei JD, Beygui RE, Zare RN. Protein-polymer hybrid nanoparticles for drug delivery. *Small* 2012;**8**:3573–8.
163. Dirks AJ, Nolte RJM, Cornelissen J. Protein-polymer hybrid amphiphiles. *Adv Mater* 2008;**20**:3953–7.
164. Marin E, Briceno MI, Caballero-George C. Critical evaluation of biodegradable polymers used in nanodrugs. *Int J Nanomed* 2013;**8**:3071–90.
165. Davis ME, Chen Z, Shin DM. Nanoparticle therapeutics: an emerging treatment modality for cancer. *Nat Rev Drug Discov* 2008;**7**:771–82.
166. Shimanovich U, Bernardes GJL, Knowles TPJ, Cavaco-Paulo A. Protein micro- and nano-capsules for biomedical applications. *Chem Soc Rev* 2014;**43**:1361–71.
167. Feng Q, Sun JS, Jiang XY. Microfluidics-mediated assembly of functional nanoparticles for cancer-related pharmaceutical applications. *Nanoscale* 2016;**8**:12430–43.
168. Jeon HJ, Lee CY, Kim MJ, Nguyen XD, Park DH, Kim HH, et al. Preparation of protein nanoparticles using NTA end functionalized polystyrenes on the interface of a multi-laminated flow formed in a microchannel. *Micromachines* 2017;**8**:10.
169. Shin S, Kim N, Hong JW. Comparison of surface modification techniques on polydimethylsiloxane to prevent protein adsorption. *BioChip J* 2018;**12**:123–7.
170. Hakala TA, Davies S, Toprakcioglu Z, Bernardim B, Bernardes GJL, Knowles TPJ. A microfluidic co-flow route for human serum albumin-drug-nanoparticle assembly. *Chemistry* 2020;**26**:5965–9.
171. Reis CP, Neufeld RJ, Ribeiro AJ, Veiga F, Nanoencapsulation I. Methods for preparation of drug-loaded polymeric nanoparticles. *Nanomedicine* 2006;**2**:8–21.
172. Meyer RA, Green JJ. Shaping the future of nanomedicine: anisotropy in polymeric nanoparticle design. *Wiley Interdiscip Rev Nanomed Nanobiotechnol* 2016;**8**:191–207.
173. Yang GZ, Liu Y, Jin S, Zhao CX. Development of core-shell nanoparticle drug delivery systems based on biomimetic mineralization. *ChemBiochem* 2020;**21**:2871–9.
174. Liberman A, Mendez N, Trogler WC, Kummel AC. Synthesis and surface functionalization of silica nanoparticles for nanomedicine. *Surf Sci Rep* 2014;**69**:132–58.
175. Jeelani PG, Mulay P, Venkat R, Ramalingam C. Multifaceted application of silica nanoparticles. A review. *Silicon* 2020;**12**:1337–54.
176. Dizaj SM, Lotfipour F, Barzegar-Jalali M, Zarrintan MH, Adibkia K. Antimicrobial activity of the metals and metal oxide nanoparticles. *Mater Sci Eng C-Mater Biol Appl* 2014;**44**:278–84.

177. Gao CB, Lyu FL, Yin YD. Encapsulated metal nanoparticles for catalysis. *Chem Rev* 2021;**121**:834–81.
178. Sengul AB, Asmatulu E. Toxicity of metal and metal oxide nanoparticles: a review. *Environ Chem Lett* 2020;**18**:1659–83.
179. Babu LT, Paira P. Current application of quantum dots (QD) in cancer therapy: a review. *Mini-Rev Med Chem* 2017;**17**:1406–15.
180. Tengjisi Hui Y, Yang GZ, Fu CK, Liu Y, Zhao CX. Biomimetic core-shell silica nanoparticles using a dual-functional peptide. *J Colloid Interface Sci* 2021;**581**:185–94.
181. Liu SW, Wang L, Lin M, Liu Y, Zhang LN, Zhang H. Tumor photothermal therapy employing photothermal inorganic nanoparticles/polymers nanocomposites. *Chin J Polym Sci* 2019;**37**:115–28.
182. Wang FL, Li CY, Cheng J, Yuan ZQ. Recent advances on inorganic nanoparticle-based cancer therapeutic agents. *Int J Environ Res Publ Health* 2016;**13**:1182.
183. Luther DC, Huang R, Jeon T, Zhang XZ, Lee YW, Nagaraj H, et al. Delivery of drugs, proteins, and nucleic acids using inorganic nanoparticles. *Adv Drug Deliv Rev* 2020;**156**:188–213.
184. Zhou YX, Quan GL, Wu QL, Zhang XX, Niu BY, Wu BY, et al. Mesoporous silica nanoparticles for drug and gene delivery. *Acta Pharm Sin B* 2018;**8**:165–77.
185. Liang RZ, Wei M, Evans DG, Duan X. Inorganic nanomaterials for bioimaging, targeted drug delivery and therapeutics. *Chem Commun* 2014;**50**:14071–81.
186. Kim CS, Tonga GY, Solfiell D, Rotello VM. Inorganic nanosystems for therapeutic delivery: status and prospects. *Adv Drug Deliv Rev* 2013;**65**:93–9.
187. Amreen K, Goel S. Review-miniaturized and microfluidic devices for automated nanoparticle synthesis. *ECS J Solid State Sci Technol* 2021;**10**:017002.
188. Le NHA, Phan HV, Yu JQ, Chan HK, Neild A, Alan T. Acoustically enhanced microfluidic mixer to synthesize highly uniform nanodrugs without the addition of stabilizers. *Int J Nanomed* 2018;**13**:1353–9.
189. Baby T, Liu Y, Middelberg APJ, Zhao CX. Fundamental studies on throughput capacities of hydrodynamic flow-focusing microfluidics for producing monodisperse polymer nanoparticles. *Chem Eng Sci* 2017;**169**:128–39.
190. Li Z, Tan B, Allix M, Cooper AI, Rosseinsky MJ. Direct coprecipitation route to monodisperse dual-functionalized magnetic iron oxide nanocrystals without size selection. *Small* 2008;**4**:231–9.
191. Panariello L, Wu GW, Besenhard MO, Loizou K, Storozhuk L, Thanh NTK, et al. A modular millifluidic platform for the synthesis of iron oxide nanoparticles with control over dissolved gas and flow configuration. *Materials* 2020;**13**:1019.
192. Le NHA, Deng H, Devendran C, Akhtar N, Ma XM, Pouton C, et al. Ultrafast star-shaped acoustic micromixer for high throughput nanoparticle synthesis. *Lab Chip* 2020;**20**:582–91.
193. Gunther A, Khan SA, Thalmann M, Trachsel F, Jensen KF. Transport and reaction in microscale segmented gas-liquid flow. *Lab Chip* 2004;**4**:278–86.
194. Khan SA, Gunther A, Schmidt MA, Jensen KF. Microfluidic synthesis of colloidal silica. *Langmuir* 2004;**20**:8604–11.
195. He P, Greenway G, Haswell SJ. Microfluidic synthesis of silica nanoparticles using polyethylenimine polymers. *Chem Eng J* 2011;**167**:694–9.
196. Liu DF, Zhang HB, Makila E, Fan J, Herranz-Blanco B, Wang CF, et al. Microfluidic assisted one-step fabrication of porous silicon@acetalated dextran nanocomposites for precisely controlled combination chemotherapy. *Biomaterials* 2015;**39**:249–59.
197. Trewyn BG, Slowing II, Giri S, Chen HT, Lin VSY. Synthesis and functionalization of a mesoporous silica nanoparticle based on the sol-gel process and applications in controlled release. *Acc Chem Res* 2007;**40**:846–53.
198. Wen J, Yang K, Xu YQ, Li HJ, Liu FY, Sun SG. Construction of a triple-stimuli-responsive system based on cerium oxide coated mesoporous silica nanoparticles. *Sci Rep* 2016;**6**:38931.
199. Yan JQ, Xu XY, Zhou JN, Liu C, Zhang LR, Wang DQ, et al. Fabrication of a pH/redox-triggered mesoporous silica-based nanoparticle with microfluidics for anticancer drugs doxorubicin and paclitaxel codelivery. *ACS Appl Bio Mater* 2020;**3**:1216–25.
200. Kucukturkmen B, Inam W, Howaili F, Gouda M, Prabhakar N, Zhang HB, et al. Microfluidic-assisted fabrication of dual-coated pH-sensitive mesoporous silica nanoparticles for protein delivery. *Biosensors* 2022;**12**:181.
201. Baber M, Mazzei L, Thanh NTK, Gavriilidis A. An engineering approach to synthesis of gold and silver nanoparticles by controlling hydrodynamics and mixing based on a coaxial flow reactor. *Nano-scale* 2017;**9**:14149–61.
202. Patil GA, Bari ML, Bhanvase BA, Ganvir V, Mishra S, Sonawane SH. Continuous synthesis of functional silver nanoparticles using microreactor: effect of surfactant and process parameters. *Chem Eng Process* 2012;**62**:69–77.
203. Hao NJ, Nie Y, Xu Z, Zhang JXJ. Ultrafast microfluidic synthesis of hierarchical triangular silver core-silica shell nanoplatelet toward enhanced cellular internalization. *J Colloid Interface Sci* 2019;**542**:370–8.
204. Zhang WW, Zhao XX, Yuan Y, Miao FL, Li WG, Ji SX, et al. Microfluidic synthesis of multimode Au@CoFeB-Rg3 nanomedicines and their cytotoxicity and anti-tumor effects. *Chem Mater* 2020;**32**:5044–56.
205. Horcajada P, Chalati T, Serre C, Gillet B, Sebrie C, Baati T, et al. Porous metal-organic-framework nanoscale carriers as a potential platform for drug delivery and imaging. *Nat Mater* 2010;**9**:172–8.
206. Wang L, Zheng M, Xie ZG. Nanoscale metal-organic frameworks for drug delivery: a conventional platform with new promise. *J Mater Chem B* 2018;**6**:707–17.
207. Rohra N, Gaikwad G, Dandekar P, Jain R. Microfluidic synthesis of a bioactive metal-organic framework for glucose-responsive insulin delivery. *ACS Appl Mater Interfaces* 2022;**14**:8251–65.
208. Akinc A, Maier MA, Manoharan M, Fitzgerald K, Jayaraman M, Barros S, et al. The Onpatro story and the clinical translation of nanomedicines containing nucleic acid-based drugs. *Nat Nanotechnol* 2019;**14**:1084–7.
209. Sealy A. Manufacturing moonshot: how Pfizer makes its millions of COVID-19 vaccine doses. Accessed: October 2021. Available from: <https://edition.cnn.com/2021/03/31/health/pfizer-vaccine-manufacturing/index.html>.
210. StemiRNA Therapeutics Co., Ltd. A globally differentiated mRNA platform starting from the new crown vaccine, strategically deploying the next generation of immunotherapy drugs. Accessed: February 2022. Available from: <https://www.stemirna.com/news/info.aspx?itemid=150>.
211. StemiRNA Therapeutics Co., Ltd. The first mRNA personalized tumor vaccine in China has entered the overseas clinical stage, from StemiRNA Therapeutics! Accessed: February 2022. Available from: <https://www.stemirna.com/news/info.aspx?itemid=164>.
212. Akso Biotechnology. Accessed: February 2022. Available from: <https://www.akso-biotech.com/newsinfo/2279106.html>.